

Sedimentary and structural evolution of a relict subglacial to subaerial drainage system and its hydrogeological implications: an example from Anglesey, north Wales, UK

Jonathan R. Lee^{1*}, Oliver J. W. Wakefield¹, Emrys Phillips², Leanne Hughes¹

¹British Geological Survey, Keyworth, Nottingham, NG12 5GG, UK.

²British Geological Survey, West Mains Road, Edinburgh, EH9 3LA, UK.

*Corresponding Author: J.R. Lee (email: jrlee@bgs.ac.uk)

Abstract

Subglacial drainage systems exert a major control on basal-sliding rates and glacier dynamics. However, comparatively few studies have examined the sedimentary record of subglacial drainage. This is due to the paucity of modern analogues, the limited recognition and preservation of upper flow regime deposits within the geological record, and the difficulty of distinguishing subglacial meltwater deposits from other meltwater sediments (e.g. glacier outburst flood deposits). Within this study, the sedimentological and structural evolution of a subglacial to subaerial (ice-marginal / proglacial) drainage system is examined. Particular emphasis is placed upon the genetic development and preservation of upper flow regime bedforms and specifically recognising them within a subglacial meltwater context. Facies attributed to subglacial meltwater activity record sedimentation within a confined, but progressively enlarging, subglacial channel system produced under dune to upper flow regime conditions. Bedforms include rare large-scale sinusoidal bedding with syn-depositional deformation produced by current-induced traction and shearing within the channel margins. Subglacial sedimentation culminated with the abrupt change to a more ephemeral drainage regime indicating channel-abandonment or a seasonal drainage regime. Retreat of the ice margin, led to the establishment of subaerial drainage with phases of sheet-flow punctuated by channel incision and anastomosing channel development under diurnal, ablation-related, seasonal discharge. The presence of extensive hydrofracture networks demonstrate that proglacial groundwater-levels fluctuated markedly and this may have influenced later overriding of the site by an ice stream.

Keywords: subglacial drainage; upper plane bed; helicoidal flow; sinusoidal bedding; hydrofracturing; groundwater

Highlights

- This paper describes subglacial and subaerial meltwater sediments.
- Meltwater bedforms include large-scale sinusoidal bedding (upper flow regime).
- Hydrofracture development indicates fluctuating groundwater conditions.
- Preservation mechanism for upper flow regime bedforms outlined.

Lee, J.R., Wakefield, O.J.W., Phillips, E. & Hughes, L. 2015. Sedimentary and structural evolution of a relict subglacial to subaerial drainage system and its hydrogeological implications: an example from Anglesey, north Wales, UK. *Quaternary Science Reviews* 109, 88-105. [ACCEPTED MANUSCRIPT]

- Criteria for distinguishing subglacial meltwater deposits.

1. Introduction

Glacial meltwater systems occur beneath many contemporary ice-masses and have been widely interpreted from past episodes of glaciation (Ehlers, 1990; Piotrowski, 1997; Benn & Evans, 2010). Understanding the behaviour of subglacial meltwater systems is crucial because of their influence upon substrate rheology and ice-bed coupling (Boulton & Hindmarsh, 1987; Iverson *et al.*, 1995; Boulton, 1996; Piotrowski *et al.*, 2004, 2006; Evans *et al.*, 2006; Kjær *et al.*, 2006; Lee & Phillips, 2008; Boulton *et al.*, 2009), and in-turn, glacier dynamics that operate over a range of temporal and spatial scales (Kamb, 1987; Bartholomew *et al.*, 2010; Sundal *et al.*, 2011; Robel *et al.*, 2013). Research now recognises that these processes act to drive the expansion, break-up and collapse of major ice streams and ice masses (MacAyeal, 1993; Clark, 1994; Tulaczyk *et al.*, 2000; Bell *et al.*, 2007; Stokes *et al.*, 2007; Burke *et al.*, 2012) thus linking subglacial drainage to collapsing ice masses, sea-level change and abrupt climate change (Goezler *et al.*, 2011; King *et al.*, 2012; Hanna *et al.*, 2013; Fürst *et al.*, 2014 and references therein). Indeed, subglacial meltwater systems underpin major global issues surrounding the stability of the modern Antarctic and Greenland ice sheets, their sensitivity too and influence on current and future changes in sea-level and climate (Alley *et al.*, 2005; Zwally *et al.*, 2005; Shepherd & Wingham, 2007; Pfeffer *et al.*, 2008).

Improving knowledge of the meltwater processes that operate within the subglacial environment – and particularly ‘channelised’ drainage, is an important but highly-problematic challenge. Modern subglacial drainage systems are largely inaccessible to all but indirect methods such as geophysical, geochemical and monitoring techniques (Hodgkins, 1997; Dowdeswell & Siegert, 2003; Rippin *et al.*, 2003; Bingham *et al.*, 2005; Smith *et al.*, 2009). Studies centred upon the geological record or recently deglaciated areas have focussed primarily upon evidence derived from the landform record (Dahl, 1965; Röthlisberger, 1972; Nye, 1973; Walder, 1986, 2010; Kamb *et al.*, 1985; Fowler, 1987; Kamb, 1987; Wingfield, 1990; Brennand & Shaw, 1995; Ó Cofaigh, 1996; Piotrowski, 1997).

Sedimentary evidence for subglacial drainage networks has proven more elusive. This is because of the lack of suitable modern analogues (Benn & Evans, 2010), the inherent low preservation potential of upper flow regime bedforms, their limited recognition and classification, and occurrence within a range of other geological settings (Fielding, 2006). Consequently, research in glacial environments has generally targeted deposits that form prominent sediment-landform assemblages such as eskers and tunnel valleys (Shreve, 1985; Brennand, 1994; Clark & Walder, 1994; Warren & Ashley, 1994; Delaney, 2001, 2002). Studies relating to smaller meltwater features, or those that possess a more subtle or no surface expression, have proven more difficult to recognise and interpret for the reasons given above, but several studies have been published (Piotrowski & Tulaczyk, 1999; Piotrowski *et al.*, 1999; Fisher *et al.*, 2003; Evans *et al.*, 2005; Phillips & Lee, 2013).

This study provides a rare and unique opportunity to examine the sedimentology and structural evolution of a relict subglacial to subaerial (proglacial) drainage system located in Anglesey, north Wales, UK. Sediments and bedforms reveal a progressively-expanding subglacial drainage system and a late-stage switch in hydrogeological regime to subaerial discharge during ice-marginal retreat. The importance of a fluctuating groundwater system is highlighted by the development of several hydrofracture networks that document the cyclical build-up and rapid release of elevated porewater

Lee, J.R., Wakefield, O.J.W., Phillips, E. & Hughes, L. 2015. Sedimentary and structural evolution of a relict subglacial to subaerial drainage system and its hydrogeological implications: an example from Anglesey, north Wales, UK. *Quaternary Science Reviews* 109, 88-105. [ACCEPTED MANUSCRIPT]

pressures within the ice-marginal to proglacial environment. Particular emphasis is placed upon exploring the development and preservation of upper flow regime bedforms and identifying criteria to establish a subglacial genesis.

2. Background and Methodology

2.1 Location of study area and Quaternary context

This study area is located adjacent to Lleiniog (National Grid Reference (NGR): SH 6200,7920) near Beaumaris on the east coast of Anglesey, north Wales, UK (Figure 1a, b). The region around Lleiniog is low-lying (<25m O.D.) and bordered to the east by the Menai Strait which separate Anglesey from mainland Wales. Bedrock strata underlying the study area comprises inter-bedded sandstones and mudstones of Ordovician age (Figure 1a). To the north these rocks are unconformably overlain by the Carboniferous Cefn Mawr Limestone Formation (Figure 1a) that form the prominent headland around Penmon and Puffin Island.

The Quaternary deposits of Anglesey form a thin and discontinuous veneer that mantles the bedrock. The most prominent superficial deposit is a diamicton containing far-travelled erratic lithologies sourced from bedrock strata within and surrounding Irish Sea Basin. This diamicton is synonymous with the 'Irish Sea till' (Greenly, 1919; Campbell & Bowen, 1989; Williams, 2003; Thomas & Chiverrell, 2007; Phillips *et al.*, 2010) which forms part of the Irish Sea Coast Subgroup of the Caledonia Glacigenic Group (McMillan & Merritt, 2012). The till was deposited extensively around the Irish Sea Basin by the Irish Sea Ice Stream during the Late Weichselian (Devensian; MIS 2) glaciation (Figure 1c). The overriding of Anglesey and the adjacent offshore area by the Irish Sea Ice Stream led to the sculpting of the substrate and development of streamlined bedrock features (e.g., streamlined bedrock, roche moutonnée, rock-cored drumlins) and sediment- to bedrock-cored (e.g. drumlins) subglacial bedforms (Hart 1995; Thomas & Chiverrell, 2007; van Landeghem *et al.*, 2009; Phillips *et al.*, 2010). These landforms and locally-preserved glacial striae record an overall ice-movement direction from northeast to southwest across Anglesey. The Irish Sea Ice Stream was one of several ice streams that drained the interior of the last British Irish Ice Sheet (Figure 1c) (Evans *et al.*, 2005; Bradwell *et al.*, 2008; Hubbard *et al.*, 2009; Clark, C.D. *et al.*, 2012; Clark, J. *et al.*, 2012). At its maximum extent (c.24-23 ka BP) the ice stream occupied much of the Irish Sea Basin and was fed by glaciers emanating from western Britain and eastern Ireland (Knight *et al.*, 1999; Clark & Meehan, 2001; Hiemstra *et al.*, 2006; Roberts *et al.*, 2007; Greenwood & Clark, 2009; Scourse *et al.*, 2009; Rijdsdijk *et al.*, 2010; Clark, J. *et al.*, 2012; Chiverrell *et al.*, 2013).

2.2 Methodology

Cliff and foreshore sections between Beaumaris and Trwyn y Penrhyn were examined between 2009 and 2014. An overview of the stratigraphic succession is provided within Section 3 below, but the sequence comprises two diamicton units separated by an intervening assemblage of sands and gravels – the focus of this study. Sands and gravels are subdivided into three distinctive 'lithofacies' (Lithofacies A-C) based upon geometry and bulk properties. Aerial photos, field mapping and hand-dug excavations were used to update the mapped extent and geometry of foreshore outcrops (Lithofacies A) as originally defined by Helm and Roberts (1984). Sediments that crop-out within the

cliff sections, including sands and gravels (Lithofacies B and C), allow the pseudo three-dimensional geometry of the bedforms to be visualised due to the variable orientation of the cliff face. Sediments exposed within the foreshore and cliff sections were described using standard sedimentological and structural terminology with particular attention paid to describing characteristics including colour, texture, structure (both primary and secondary tectonic) and the geometric relationships between bedding. The orientation and inclination of bedding surfaces, bounding surfaces and structural features (e.g. faults) were recorded using a compass clinometer with data plotted as either rose diagrams (palaeocurrents) or as great circles and poles to planes within lower hemisphere stereographic projections (faults).

3. Stratigraphic framework of the study area

Logging and mapping of the coastal and foreshore sections between Beaumaris and Trwyn y Penrhyn reveals a five-tiered Quaternary succession (Figure 2) enabling the sand and gravel lithofacies – the focus of this paper, to be placed within a wider stratigraphical and genetic context. The adjacent diamicton units are described briefly below whilst the sands and gravel are described within the succeeding section.

The basal (oldest) unit within the sequence, the **basal diamicton** – also called the ‘blue till’ (Greenly, 1919), crops-out discontinuously along the cliff base and foreshore (Figure 2). It exhibits a maximum observed thickness of 6m although the base was obscured. The diamicton is composed of a highly-consolidated dark grey (2.5Y 4/1) matrix-supported diamicton containing sub-angular to sub-rounded clasts (upto boulder size) of locally-derived Ordovician sandstone and mudstone and Carboniferous limestone (often striated). The diamicton was originally considered to provide evidence for the westwards expansion of Welsh mainland ice onto Anglesey (Greenly, 1919). However, the allochthonous micro-fossil assemblage contains locally-derived (Carboniferous) and further-travelled species (Devonian / Mesozoic) sourced from the floor of the Irish Sea Basin and/or northwest England (see Sample 2, Table 1, Phillips *et al.*, 2013). The unit has been reinterpreted as pre-existing regolith that has subsequently been overridden and glacitected by Irish Sea ice with the addition of a minor far-travelled component (Phillips *et al.*, 2013a).

Resting unconformably upon the basal diamicton between Tre-castell and Trwyn y Penrhyn are a 5-10 m thick sequence of **sands and gravels** (Greenly, 1919; Walsh *et al.*, 1982; Helm & Roberts, 1984). Within this study, the sands and gravels have been sub-divided into **Lithofacies A-C** and their genesis is explored below in the following sections. The sand fraction (Lithofacies B) is texturally and compositionally immature (heterolithic), and comprises angular to edge-rounded, low-sphericity sedimentary and crystalline lithic grains (Appendix 1). The clast assemblage (Lithofacies B) is dominated by locally-derived sedimentary clasts including limestone and coal (Carboniferous), sandstone and mudstone (Ordovician); with subordinate concentrations of far-travelled wacke sandstone and litharenite (Lower Palaeozoic, southwest Scotland and/or Cumbria), red mudstone, siltstone and sandstone (Devonian / Carboniferous and/or Permian, Irish Sea Basin and/or northwest England, Isle of Man) (Appendix 2). Igneous lithologies consist of granophyric granite and muscovite-biotite granite (Ennerdale and Eskdale plutons, northwest England), biotite-amphibole-granodiorite (Cairnsmore of Fleet and Criffel-Dalbeattie plutons of southwest Scotland), variably-altered fine-

Lee, J.R., Wakefield, O.J.W., Phillips, E. & Hughes, L. 2015. Sedimentary and structural evolution of a relict subglacial to subaerial drainage system and its hydrogeological implications: an example from Anglesey, north Wales, UK. *Quaternary Science Reviews* 109, 88-105. [ACCEPTED MANUSCRIPT]

grained aphyric to microporphyrific dacite-rhyolite (felsites) and rhyolitic lapilli-tuff (Borrowdale Volcanic Group, northwest England and/or Palaeogene of southern Scotland), pyroxene-plagioclase phyrific basalt (Palaeogene of southern Scotland) (Appendix 2; Figure 1c).

The **upper diamicton** is the highest glacial unit within the succession and comprises a highly-consolidated light olive brown (2.5Y 5/4) variably matrix- to clast-supported diamicton with a maximum observed thickness of 5m. It crops-out discontinuously along the coastal section and overlies either the basal diamicton or sands and gravels (Lithofacies A-C). Lithologically, the diamicton is dominated by locally-sourced Carboniferous materials including palynomorphs (Sample 5, Table 1 in Phillips *et al.*, 2013), coal fragments and limestone clasts – the latter are commonly striated and exhibit keel-shaped clast bottoms (Greenly, 1919). Subordinate proportions of mudstone (Ordovician) and red sandstone (Devonian Old Red Sandstone / Carboniferous and/or Triassic sandstone) are also evident together with clasts of greywacke (southern Scotland), quartz schist (central Scotland) and biotite-muscovite granite (?Eskdale Pluton, northwest England). The unit is synonymous with the 'Irish Sea till' (Greenly, 1919; Campbell & Bowen, 1989; Williams, 2003; Thomas & Chiverrell, 2007; Phillips *et al.*, 2010). The till was deposited extensively within and around the margins of the Irish Sea Basin by the Irish Sea Ice Stream during the Late Weichselian (Devensian; MIS 2) glaciation (Thomas & Chiverrell, 2010; Phillips *et al.*, 2010; McMillan & Merritt, 2012). Collectively, the basal and upper diamictons, together with the sands and gravels (Lithofacies A-C) contain a similar suite of local and far-travelled lithologies indicating a singular source for all of the deposits at Lleiniog.

4. Description and Interpretation of sands and gravels

4.1 Lithofacies A

Lithofacies A crops-out on the foreshore at low-tide adjacent to Trwyn y Penrhyn and more extensively in the vicinity of Lleiniog (Figure 2, 3a). It rests unconformably upon the sharp and irregular surface of the basal diamicton which dips gently (<2°) eastwards. Small excavations on the foreshore reveal that the irregular surface of the basal diamicton also exhibits several deep sediment-filled scours upto 1.4m width and 0.6m depth. The scour within cross-section Y1-Y2 exhibits a steep-sided and irregular base and is 0.5m deep (Figure 3b). Occurring at the base of the scour is a 0.1m thick basal lag constituting gravel and rip-up clasts composed of basal diamicton. This is overlain by a 0.4m thick bed of highly-consolidated matrix-supported diamicton which possesses a similar lithology to the basal diamicton but is more gravel-rich including occasional small striated and keel-shaped limestone (Carboniferous) clasts and far-travelled lithologies such as granodiorite and greywacke. The diamicton was massive with a variably-sharp to diffuse (wispy and flame-like) lower contact with the basal diamicton (Figure 3b). Overlying the diamicton is a bed of crudely-imbricated, chaotic matrix- to clast-supported, weakly carbonate-cemented greyish-brown (2.5Y 4/4) gravel. The gravel forms a convex-upwards sediment body that infills the scour and oversteps the basal diamicton.

Cross section X1-X2 shows a scour that is asymmetrical in form and possesses an irregular and undulating base marked by a thin (0.08m) basal lag containing gravel clasts and occasional rounded

rip-up clasts composed of dark grey (2/5Y 4/1) diamicton (Figure 3c). The contact between the basal lag and the overlying dish-shaped body of diamicton is sharp and sub-horizontal. The diamicton possesses a dark grey (2.5Y 4/1) colouration, is highly-consolidated, massive, matrix-supported and contains abundant locally-derived angular clasts. Cut into the diamicton unit is a 0.45m thick lenticular-shaped unit of greyish brown (2.5Y 4/4) gravel. This gravel infills the remainder of the scour and exhibits a sharp and undulatory lower contact, laterally dissecting the original sub-vertical scour margin (Figure 3c). Compositionally and structurally, the gravel is identical to the scour observed in cross section X1-X2 except that it contains sporadic thin (<4mm) lenses of coarse sand. The upper bounding surface of the gravel body is convex-upwards and similarly to the previous scour-fill, extends vertically and laterally beyond the margins of the scour. Mapping of the foreshore shows that the upper gravel units within both cross-sections form ribbon-like aggradations that can be traced northwards for tens of metres where they form the cores to distinctive landforms described below (Figure 3a). Other gravel cores – albeit unexcavated, possess a similar geometric relationship to landforms that crop-out on the foreshore (Figure 3a).

The sharp and irregular surface morphology of the basal diamicton is consistent with scour and dissection by high-energy tractive currents (Miall, 1985). These currents are interpreted as incising the deep scours (cross-sections X1-X2 and Y1-Y2) and ripping-up and reworking beds of the basal diamicton which were deposited together with the gravel as a basal lag. Overlying beds of diamicton record an abrupt switch in sedimentation. The absence of normal faulting and parasitic folding preclude the diamicton from being formed by collapse of material forming the scour walls. Instead, the high consolidation of the diamicton, the presence of clasts from local and far-travelled sources plus the striated and keel-shaped limestone clasts are suggestive of subglacial till accretion (cf. Boulton & Paul, 1976; Lian *et al.*, 2003; Benn & Evans, 2010). Flame-like margins along the base of the diamicton unit (Y1-Y2 scour) imply rapid loading and dewatering of the underlying basal lag. The upper contacts of the diamicton units with the overlying lenticular-shaped gravel bodies are sharp and erosional. Erosion was the product of high-energy tractive currents (Miall, 1985) largely driving vertical incision, but the geometry of the gravel base within section Z1-Z2 also demonstrates lateral erosion and widening of the scour. Deposition of the gravel from bedload saltation occurred under a relatively low-viscosity turbulent flow (Leeder, 2011) with thin sand lenses recording temporary reductions in flow regime. The mapped occurrence of these gravels (Figure 3a) indicates that they - and by inference the scours, form part of a more extensive channel network with deep-scouring focussed into discrete channelised zones. The convex-up morphology of the upper bounding surfaces which rise above the confines of the channels, imply that flow was laterally constrained enabling bedform aggradation.

Gravel bodies form the cores of linear, straight to curved sand ridges that can be traced along the foreshore at Lleiniog (Figure 3a). They possess wavelengths of upto 6m and are separated by troughs upto 1m deep with long-axes orientated broadly northeast-southwest. In cross-section, ridges comprise the gravel cores described above, overlain by cross-bedded gravelly sand which grade both vertically and laterally into coarse sands. Individual cross-sets forming the ridge crests drape the flanks of the ridges, thinning and dipping southwards indicating bedform migration towards the south. Bedding thickens progressively down the ridge flanks into the troughs, where bedding set boundaries strike parallel or slightly obliquely to the ridge axes. The lateral margins of these ridges

exhibit a complex inter-fingering relationship with adjacent ridges (Figure 4a,b). This relationship isn't only confined to the middle portion of the inter-ridge trough and was also observed by the onlapping of toesets from adjacent ridges. As such, the margins of these ridges appear feathered and can be hard to ascertain when not well exposed.

Helm & Roberts (1982) interpreted these geometric relationships as denoting reactivation surfaces. However, using a strict definition of the term (*sensu* McCabe & Jones, 1977), they are now considered to represent bounding surfaces formed in response to the interaction and competition for available accommodation space by two adjacent (coeval) laterally accreting bedforms. The internal morphology of these bedforms suggests that while they were down-flow accreting by slip-face avalanching, they were also vertically aggrading indicative of a high and sustained sediment supply. Furthermore, the longitudinal morphology of these bedforms suggests that they developed as a result of helicoidal (longitudinal) flow (Folk, 1976; Leeder, 2011). The sinuosity observed in some of the bedforms, suggests that the helicoidal vortices were either: (i) stable (fixed) and had a degree of sinuosity to them; or (ii) were variable and moved laterally producing variably-shaped bedforms; or (iii) could represent a transition from transverse vortices into nearly elongate and straight longitudinal flows (Folk, 1976).

4.2 Lithofacies B

Lithofacies B crops-out at the base of the cliffs at Lleiniog and can be traced discontinuously southwards towards Gored-bach where it reaches a maximum observed thickness of 6m although the base was obscured by modern beach material (Figure 5). It is lithologically similar to the gravels within Lithofacies A, comprising carbonate-cemented, greyish brown (2.5Y 5/2) clast-supported gravels passing upwards into medium-coarse grained sands. Coarse gravels dominate the lithofacies between 87-109m and fine laterally towards both the southeast and northwest. Clasts possess varying degrees of edge-rounding and angularity with the long axis of elongate clasts typically aligned parallel to bedding surfaces (Figure 4c). No obvious imbrication was observed.

Bedding is defined by subtle variations in particle size and sorting (Figure 4c). It forms a series of broadly-symmetrical bedforms along their short-axes that possess wavelengths of between 4-10m and amplitudes of 1-3m that can be traced laterally for up to 30m (Figure 4d, 4e, 5). These bedforms are aligned slightly oblique to the trend of the cliff-line in a broadly north-south orientation. They are straight-crested linear (parallel to palaeoflow) features with a very low degree of along-flow sinuosity (sinuosity to straight-line length ratio of near 1:~1) and possess similar gross-scale geometries as the ridges of Lithofacies A. Internally however, Lithofacies B bedforms differ from those of Lithofacies A as they comprise parallel to sub-parallel bedding surfaces that can be traced laterally for several tens of metres through several troughs and crests with both lee- and stoss-side preservation (Figure 5). In detail, two types of bedding have been recognised: Type 1 where individual beds maintain a uniform thickness (<0.1m thick) between ridge crests and adjacent troughs (e.g. between 55-75m and 87-126m on Figure 5); and Type 2 in which bedding in one ridge is truncated by onlapping beds from adjacent bedform with bedding on the truncated limbs often thinning away from the crests (e.g. 180-200m on Figure 5). Type 1 beds form stacked sets that are almost perfectly in-phase with crests and troughs of overlying beds (see Figures 5) with no indication of subsequent lateral bed movement.

Lee, J.R., Wakefield, O.J.W., Phillips, E. & Hughes, L. 2015. Sedimentary and structural evolution of a relict subglacial to subaerial drainage system and its hydrogeological implications: an example from Anglesey, north Wales, UK. *Quaternary Science Reviews* 109, 88-105. [ACCEPTED MANUSCRIPT]

The slopes either side of the crestline are symmetrical with dips commonly $\sim 10^\circ$ and slope lengths of $\sim 3\text{-}4\text{m}$ from crest to trough. Bedform crestlines are sub-horizontontal to gently dipping ($<2^\circ$) in a down-current direction (between southwest to southeast).

Based upon the morphology and geometry of the bedforms and their internal structure, these structures are interpreted as large-scale sinusoidal bedforms (Fielding, 2006; Ito, 2010; Lang & Winsemann, 2013). The geometry of the bedforms is similar to supercritical 'sinusoidal ripples', albeit at a dune scale, which are produced by rapid and high rates of deposition from near-bed suspension (Jopling & Walker, 1968; Allen, 1973; Fielding, 2006), with inter-bed variations in particle size recording subtle changes in flow regime and bedload transportation (Leeder, 2011). An alternative interpretation of these unusual structures as tectonically-derived folds also requires consideration. However, a tectonic origin is discounted due to the absence of distinctive evidence for deformation produced by sediment loading (e.g. disharmonic folding, tight to closed fold limbs, flame-like bed contacts; cf. Kelling & Walton, 1957; Owen, 1996, 2003) and glacitectonic 'pushing' (e.g. open folding exhibiting axial-planar cleavage, parasitic folding and hinge-faulting; cf. Benn & Prave, 2006; Benediktsson *et al.*, 2010; Lee *et al.*, 2013). Similar to Lithofacies A, the longitudinal morphology of the ridge-like bedforms of Lithofacies B suggests that they are the product of helicoidal vortices associated with the upper flow regime (Folk, 1976). In such a scenario the bedform crests would have formed at the junction of the 'upward' cycling margin of adjacent out-of-phase helicoidal vortex, with troughs generated at the downward cycling junction.

Between 27-38m (Figure 5) the typically coarse-grained sediments of Lithofacies B also contain horizontally-laminated, cross-bedded and rippled fine sand, with mud drapes (Figure 4f) and coal-rich laminae (Figure 4g) recording periods of lower-energy deposition including slack-water sedimentation (Allen, 1980). In places, bedding within the sands has been disrupted by small-scale deformation structures including sets of recumbent and conjugate folds with fold axes aligned broadly parallel / sub-parallel to bedding (Figure 4h). Folding is overlain in-turn by undeformed sediments indicating that deformation was syn-sedimentary. Conjugate folds form sub-parallel to oblique to the principal stress axes and their geometry reflect subtle shifts in the orientations of the primary stress field (Ramsay, 1962). These folds are interpreted to be the product of high shear stresses produced by sand-laden high-velocity currents flowing over liquefied sediment (Røe, 1987; Røe and Hermansen, 2006).

Elsewhere, bedding has been disturbed by reverse (Figure 4i) and extensional faulting and these can be observed to cross-cut (i.e. post-date) the earlier folding described above. Reverse faults dip $10\text{-}22^\circ$ towards the northwest, north and northeast (Figure 6a) with throws of upto 0.15m. They are truncated and overlain by later bedding demonstrating that compressive stresses were being applied during sedimentation. By contrast, normal faults exhibit a much greater variance in dip azimuth direction and inclination, with throws of upto 0.2m plunging at angles of between $20\text{-}66^\circ$ (Figure 6a). Extensional faulting probably developed to accommodate the compressional stresses being applied elsewhere to the sediments. However, faults infilled by thin sand laminae could also signify localised liquefaction driven by sediment loading and compaction (Lowe, 1975).

4.3 Lithofacies C

Lithofacies C comprises a 1 to 4m thick sequence of reddish brown (5YR 5/4) sands and gravels which overlie Lithofacies B (Figure 5). The gravels are composed predominantly of locally-sourced sub-angular to sub-rounded clasts of sandstone (Carboniferous and / or Ordovician), limestone (Carboniferous), with subordinate quantities of mudstone, chert (black) and coal.

Lithofacies C is only exposed locally between Lleiniog and Gored-bach due to it being cut-out by the irregular erosive base of the overlying upper diamicton (Figure 5). The base of this lithofacies is either conformable (Figure 4j), with sands and gravels draping and infilling the surface morphology of the underlying Lithofacies B bedforms (e.g. between 110-150m on Figure 5), or erosional with Lithofacies C infilling broad, shallow channel scours that range between 14-25m width and 3m depth (Figure 4k; 94-144m on Figure 5). These relationships are consistent with rapid burial of Lithofacies B by sediment-laden traction currents leading to localised scouring and incision (Miall, 1985; Kraus & Middleton, 1987). A number of broad (upto 55m and relatively shallow (<3m) sand and gravel-filled channels can be observed (e.g. 93-147m on Figure 5). They are infilled by poorly-sorted, massive to chaotically-bedded gravel which in-turn are cross-cut by undulatory second-order and minor bounding surfaces. These bounding surfaces reflect lateral channel migration and incision during phases of active flow (Cant & Walker, 1976; Miall, 1985, 1996).

A wide range of facies occur within Lithofacies C. They are dominated by cobble and gravel-rich units with occasional boulder horizons which overall, fine-upwards into stratified sands and gravelly sands. This general fining-upwards reflects a vertical reduction in coarse gravel supply and energy regime. Beds of massive to crudely-imbricated open-framework gravel (Figure 4j, k) are common within the lower horizons with bedding distinguished by subtle changes in clast size. Open framework gravels are thought to reflect rapid deposition from bedload under a high but variable (lower) flow regime with the continued entrainment or winnowing of fines (Maizels, 1993). Localised normal and inverse grading (cobbles-medium sand) is common and records successive stages of waning and rising flow (Miall, 1978, 1985). Occasional boulder horizons record transportation and deposition during peak flow conditions. Imbricated and massive fine gravels, plus horizontal and massive coarse sands probably record lower-stage plane beds and flow across bar-tops (Miall, 1978). Gravels pass vertically into horizontal, planar and trough cross-bedded or laminated gravelly-sands and medium-coarse sands with low-angle (3-16°) foresets dipping towards the south-southeast, south and southwest (Figure 6b). The cross-bedding formed as a result of the down-current migration of straight-crested and sinuous subaqueous sand bedforms with the channels, whilst the horizontal-bedded fine-medium sand records upper-stage plane bed flow across bar-surfaces.

At various locations along the coastal section individual sand and gravel beds have been locally-deformed. For example at 64m (Figure 5), a sand bed forms a large flame structure inter-folded with overlying gravel beds (Figure 4j). Evidence for soft sediment deformation such as these flame structures indicate that some sand units were water-saturated and became part-fluidised and mobile by rapid loading of overlying gravel units (Lowe, 1975). Critically, zones deformed by this small-scale deformation are overlain by horizons exhibiting undeformed sediments so this deformation is considered to be syn-depositional.

4.4 Meso-scale deformation structures

At Lleiniog the sediments of Lithofacies B and C are locally cross-cut by sediment-filled hydrofractures and/or deformed by brittle faults.

4.4.1 Hydrofractures and small-scale sediment-lined normal faults

Well-developed sediment-filled hydrofractures have been recognised at two sites (sites A and B; Figures 7a, b, respectively). At the first site, site A (4m, Figure 4), the stratified silts and sands of Lithofacies B are cut by a 1.8m long steeply-inclined (35-52° south), upwards tapering fracture (AF1) filled by weakly laminated to massive reddish brown (2.5Y 4/2) sand and dark greyish brown (2.5Y 4/2) sandy silt (Figure 7a). The stratification within this fill occurs parallel to sub-parallel to the margins of the fracture, consistent with either the pulsed injection of sediment-laden fluid upwards through the fracture, or repeated reactivation of this hydrofracture system (van der Meer *et al.*, 1999, 2009; Phillips & Merritt, 2008; Phillips *et al.*, 2012). The margins of the hydrofracture vary from sharp to diffuse; the latter potentially resulting from the infiltration of water and sediment into the adjacent walls of the fracture. The 'lower' end of the hydrofracture terminates at the top of a sand and gravel bed (Figure 7a). Its upper end is truncated at the base of the overlying Upper Diamicton (see Figure 5), indicating that hydrofracturing at this locality pre-dated the deposition of this unit.

Similar sediment-filled hydrofractures as well as several sediment-lined, small-scale (maximum displacement of a few 10's cm) normal (extensional) faults occur at the second site, Site B (30m on Figure 5), where they deform both Lithofacies B and C. Two sets of faults have been recognised; the first set dips steeply towards the north (down throw to the north) and a second steeply northerly dipping set (down throw to the south). Both sets of sediment-lined faults (labelled BF1 on Figure 7b) clearly offset the boundary between bedded sands of Lithofacies B and overlying Lithofacies C gravels, indicating that faulting post-dated the deposition of at least the lower part of Lithofacies C. The extensional nature of the faulting would have allowed the escape of sediment-bearing fluids from the underlying sands, leading to the deposition of a thin (<5mm) layer of sandy sediment along these faults. Lower in the section at Site B, within the Lithofacies B sands, the sediment-lined faults are locally cross-cut by a set of moderate to steeply (30-65°) southerly dipping, variably sediment-filled fractures (labelled BF2 on Figure 7b). In detail, however, the relationships between the faults and sediment-filled fractures are locally more complex, with several of the fractures appearing to 'merge' or 'link' into the earlier developed faults. Unlike the faults, however, these sediment-filled fractures do not offset bedding within the host Lithofacies B sands. The fractures are typically defined by a single planar to slightly irregular dislocation and are filled by unstratified to crudely-bedded coarse to medium sand. In one example, however, the fracture splits into an irregular network of smaller, locally diffuse sediment-filled structures forming a complex zone of brittle deformation at the end of this hydrofracture. Both the faults and fractures are cross-cut by a wide, relatively younger sand and gravelly sand-filled hydrofracture (BF3 on Figure 7b). Over much of its length (traced laterally for at least 1.5m), this 17 to 39cm wide hydrofracture cross-cuts bedding within the Lithofacies B sands, dipping at 30-45° towards the south. However, at its southern end it becomes much narrower (up to 3cm thick) and appears to have been injected along bedding within the host sands.

Such structures provide a clear record of fluctuating hydrostatic pressure, leading to brittle fracturing of the host sediment and/or bedrock, and penecontemporaneous liquefaction and introduction of

the sediment-fill. The cross-cutting relationships displayed by the hydrofractures and spatially related sediment-lined faults cutting the Lithofacies B and C at Lleiniog indicate that hydrostatic pressures repeatedly exceeded the cohesive strength of the host sediments. Furthermore, the stratified nature of the sediments filling the hydrofractures indicate that they may have been active over a prolonged period and probably accommodated several phases of fluid flow (cf. Phillips *et al.*, 2012). The relationships shown at Site A clearly indicating that hydrofracturing pre-dated the deposition of the overlying Upper Diamicton, suggesting that fluctuations in the hydrostatic pressure may have accompanied deposition of the sands and gravels; possibly partially driven by the rapid deposition of these high-energy, coarse grained sediments with compaction leading to syn-sedimentary faulting and dewatering of the sequence as a result of hydrofracturing.

4.4.2 Syn-sedimentary faulting and collapse

The most pervasive deformation observed at Lleiniog occurs at Site C (between 70-82m on Figure 5), where the Lithofacies C sands and gravels have been down-faulted into sand beds within Lithofacies B (Figure 7c). At the southern end of the site a 10m wide channel composed of Lithofacies C is fault-bound along its northern margin by two southerly dipping, curved to listric normal faults (downthrown to south) (CF1 and CF2 on Figure 7c). Bedding within the sands and gravels is over-steepened and crudely aligned parallel to the channel margin with faulting, leading to the tilting of bedding, probably having occurred in response to rotational failure of the relatively steep and unstable channel margin. In the centre of the channel, the bedding within sands and gravels are cross-cut by a large, branching flame-like mass of sand which contains folded beds of sand and gravel (at 68m on Figure 5). Folding within this zone is highly-disharmonic indicative of deformation of water-saturated sediments, with this soft-sediment deformation probably having occurred in response to liquefaction triggered by fault-driven collapse of the channel margin.

The northern end of Site C is dominated by a second 7m wide fault-bound structure filled by highly-disturbed, stratified Lithofacies B and C sands and gravels (between 75-82m on Figure 5). Following deposition of Lithofacies C, sands and gravels have been deformed by a tight, upright to steeply-inclined (axial-surface dipping to north) fault-bound syncline. The southern margin of this structure is sharp and marked by several steep, northerly-dipping normal faults with throws between 8 cm and 3 m (downthrow to north). The faults are locally lined by a thin (1 to 3cm thick) layer of massive to weakly stratified sand (similar to the faults observed at Site B) indicating that these extensional structures acted as fluid pathways (hydrofractures) which aided the dewatering of underlying Lithofacies B sediments. Faulting on the northern flank of the structure is more complicated comprising several sub-vertical to steeply north-dipping reverse faults as well as southerly dipping normal faults with throws of between 10cm and 1m (Figure 7c). Towards the top of the section, deformation is truncated by a shallow channel containing undeformed bedding indicating that deformation was syn-sedimentary and developed in response to the progressive rotation of the structure along individual fault-blocks due to loading or closure of underlying void space (Figure 7c).

5. Discussion

5.1 Genetic Model

Sediments and structures at Lleiniog have produced a sequence which are interpreted below within a subglacial (Lithofacies A and B) and subaerial (Lithofacies C) meltwater model. The subglacial

interpretation of Lithofacies A and B is controversial because few modern analogues of subglacial meltwater sediments exist and their identification is therefore ambiguous (Benn & Evans, 2010). Indeed, many of the facies recognised within Lithofacies A and B have also been recognised within a range of glacial environments (Maizels, 1997; Marren, 2005; Lang & Winsemann, 2013). Within the following section, a palaeoenvironmental model for the Lleiniog sequence is presented and discussed.

The base of the Quaternary sequence at Lleiniog is defined by the basal diamicton or the 'blue till' of Greenly (1919). Elsewhere on Anglesey, this unit has been interpreted as glacitectorite produced by subglacial shearing and reworking of localised pre-existing bedrock and regolith (Phillips *et al.*, 2013). This subglacial interpretation is endorsed because of the high-consolidation of the diamicton, presence of striated and keel-shaped limestone clasts and a minor far-travelled lithological component (Boulton & Paul, 1976; Lian *et al.*, 2003; Benn & Evans, 2010) observed in exposures at Beaumaris and Trwyn y Penrhyn (Section 3; Greenly, 1919). Scouring of the upper-surface of the basal diamicton to produce the deep sediment-filled scours is considered to have occurred by focussed meltwater incision of the subglacial bed. Evidence supporting a subglacial origin includes the sharp and steep-sided morphology of the scours and occurrence of a partial till-fill (identical to the basal diamicton) – features that have been recognised within other small subglacial meltwater channels elsewhere (Mathers & Zalasiewicz, 1986; Piotrowski & Tulaczyk, 1999; Piotrowski *et al.*, 1999). Incised meltwater streams are also common in proglacial areas of temperate glaciers (e.g. Evans & Twigg, 2002) however, without lateral confinement by ice-walls it is difficult to envisage how the upper bounding surfaces of the gravel fills could be elevated above the surface of the basal diamicton. This further implies that these scours were physically isolated from one-another at least initially.

Subglacial meltwater channels have been described widely in the literature and, depending on the cohesive strength of the substrate or ice relative to meltwater flow, typically incise downwards into the subglacial bed (N-Channels) or upwards into the ice (R-Channels) (Röthlisberger, 1972; Nye, 1973; Shreve, 1972, 1985; Walder, 1986, 2010). The geometry of the scours and associated sediment infills (**Lithofacies A**) at Lleiniog indicate an intermediate type (cf. Benn & Evans, 2010) with initial downcutting into the subglacial bed, followed by later-stage lateral-bed incision and upward incision into the overlying ice (Figure 8a). One possible mechanism for the switch to upward meltwater incision could be the armouring of the channel margins with gravel (Figure 8b; Little & Mayer, 1976). This would increase channel roughness, promoting gravel deposition and channel infill, with meltwater flow being focussed upwards into the ice enabling channel capacity to enlarge accommodating flow (Figure 8c). Continued ice-wall widening would enable deposition of the gravel beyond the lateral and vertical confines of the original scour margins (Figure 8d). Increasing the channel capacity would have the effect of a slight lowering of energy regime and turbulence allowing deposition of the sand and gravel. Following this rationale, it is argued that an energy drop resulted in the accretion of the sand and gravel ridge-trough system that crops-out on the foreshore, around the nuclei of the upstanding gravel bodies (Figure 9a). Sedimentation during the development of these bedforms was initially driven by vertical and lateral accretion and down-flow bedform migration under conditions of high-flow and relatively stable helicoidal currents, with a constant sediment supply. Of particular significance is the inter-fingering of cross-bedding within the inter-

Lee, J.R., Wakefield, O.J.W., Phillips, E. & Hughes, L. 2015. Sedimentary and structural evolution of a relict subglacial to subaerial drainage system and its hydrogeological implications: an example from Anglesey, north Wales, UK. *Quaternary Science Reviews* 109, 88-105. [ACCEPTED MANUSCRIPT]

ridge trough areas produced by washing-out of the ridge crests (Langford & Bracken, 1987; Røe, 1987; Miall, 1988). Firstly, this demonstrates the coalescence of adjacent bedforms which in-turn suggest the coalescence of subglacial meltwater conduits by lateral-widening and capture, and the development of an increasingly-linked subglacial channel network (Walder, 1986; Benn & Evans, 2010).

Lithofacies B is considered to reflect further channel enlargement, coalescence and increase in the capacity of the subglacial drainage network. A subglacial interpretation for Lithofacies B is supported by sedimentological continuity with the underlying lithofacies and by the presence of syn-depositional reverse (compressive) faulting generated by the transmission of compressive shear stresses from the channel margins (by ice wall creep or subglacial deformation) into the sediments – two features that would appear to preclude a proglacial origin. An englacial origin for these bedforms is also discounted because of the absence of post-depositional extensional faulting which would be produced as the sediment-pile is lowered during glacier decay (cf. Delaney, 2001, 2002). Bedding within Lithofacies B is characterised by large-scale sinusoidal bedforms that indicate elevated sedimentation rates at the dune to upper plane-bed transition (Fielding, 2006) associated with largely fixed or slightly oscillating helicoidal flows (Figure 9b) (Folk, 1976). Additional evidence for upper flow regime conditions is provided by syn-depositional conjugate and recumbent folds produced by traction-shearing of liquefied sediments by dense sediment-laden traction currents (Røe and Hermansen, 2006). The overall, fining-upwards of Lithofacies B reflect a rapid shut-down of the energy regime (Tunbridge, 1981; Mulder & Alexander, 2001). However, whilst the localised preservation of clay and coal drapes within fine sand ripples and cross-beds point to the large-scale abandonment of the subglacial channel system as a major drainage conduit, continued sediment influx implies a switch to a more ephemeral subglacial drainage system characterised by lower flow regimes and periods of slack-water deposition.

Truncation of Lithofacies B by **Lithofacies C** records an important palaeoenvironmental switch. The largely erosional base of Lithofacies C, coupled with beds of imbricated and massive gravel, the channelised sands and gravels with fining-upwards (waning-flow) sequences, record largely unconstrained flow which is more indicative of a subaerial (proglacial) braided channel system (Figure 9c) (McDonald & Banerjee, 1971; Rust, 1972a; 1972b; Miall, 1977; Gustavson & Boothroyd, 1987). Sediment facies record phases of sheet-flow meltwater discharge punctuated by anastomosing channel development typically associated with diurnal, ablation-related, seasonal discharge (Gustavson & Boothroyd, 1987; Maizels, 1993). Sedimentation rates and discharge were variable, with evidence for multiple phases of scouring and sheet flow punctuated by episodes of lateral channel migration within both large and small channels (McDonald & Banerjee, 1971; Miall, 1977). Ephemeral periods of active channel abandonment are indicated by small collapse structures along the margins of several of the channels (Fraser, 1993).

A striking feature of the Lleiniog sequence, are the meso-scale fault and hydrofracture systems developed at several sites and provide important clues to substrate conditions during sedimentation (Sites A and B). Much of the early stage extensional faulting appears to relate to the collapse of channel margins, consolidation and loading of the sediment pile during the accretion of Lithofacies C. Several fault systems have subsequently been reactivated as hydrofracture systems. The stratified fill of these hydrofracture systems, plus their cross-cutting geometries indicate multiple phases of fluid

Lee, J.R., Wakefield, O.J.W., Phillips, E. & Hughes, L. 2015. Sedimentary and structural evolution of a relict subglacial to subaerial drainage system and its hydrogeological implications: an example from Anglesey, north Wales, UK. *Quaternary Science Reviews* 109, 88-105. [ACCEPTED MANUSCRIPT]

flow associated with fluctuating porewater availability (Phillips and Merritt 2008; Phillips *et al.*, 2013b). Hydrofractures provide clear evidence for the passage of over-pressurised meltwater through glacial environments and are thought to be mainly developed in ice-marginal, sub-marginal to subglacial settings where the overburden pressure exerted by the ice leads to the required periodic over-pressurisation of the hydrogeological system (van der Meer *et al.*, 1999 2009; Roberts *et al.*, 2009; Phillips *et al.*, 2013b; Phillips & Hughes, 2014). This suggests that Lithofacies C was probably developed in an ice-marginal to proglacial setting with the periodic build-up of the hydrostatic pressures possibly reflecting a seasonal (spring-summer) increase in meltwater production. The graben-like geometry of the structure at Site C is consistent with that of a modified kettle hole (Maizels, 1992), implying the presence of buried ice within Lithofacies B (now obscured by the modern foreshore). Several studies have documented the widespread presence of buried ice and kettle structures within both contemporary and former ice-marginal to proglacial environments (Hambrey, 1984; Krüger, 1997; Evans & Twigg, 2002; Eyles *et al.*, 2003). These reflect either the buried remnants of detached glacier snouts (Ham & Attig, 1996; Evans & Rea, 1999; Everest & Bradwell, 2003), buried ice blocks detached from within englacial or subglacial meltwater channels (Benn and Evans, 2010), or by meltwater floods such as jökulhlaups (Gustavson & Boothroyd, 1987; Maizels, 1992; Fay, 2002). The localised nature of this type of collapse structure suggests that the buried ice occurred as discrete buried blocks that possibly originated from the failure of a subglacial conduit wall or roof during the deposition of Lithofacies B.

The model presented above advocates a subglacial origin for Lithofacies A and B. This interpretation is based upon the inferred palaeoenvironmental continuity with the basal diamicton (subglacial glaciectonite), the scoured surface of the basal diamicton (subglacial meltwater incision) including till-dominated infill (Lithofacies A), and the convex-upwards bounding surfaces of the scour-infill (Lithofacies A) that in-turn formed the nucleus for the accretion of longitudinal bedforms (Lithofacies A and B). Of further significance is the occurrence of syn-depositional reverse faulting within Lithofacies B suggestive of conduit wall modification by compressive stresses operating within the glacial bed or basal ice. However, individual sediment facies characteristic of upper or transitional flow regimes have also been recognised within englacial outwash sediments (Delaney, 2001, 2002) and proglacial glacier outburst flood or jökulhlaup deposits (Lord *et al.*, 1987; Maizels, 1997; Marren, 2005). An alternative 'englacial' origin is rejected here because of the overall high-degree of lateral bedding continuity which is often absent from englacial deposits due to post-depositional deformation produced by lowering during mass-wastage (cf. Delaney, 2001, 2002). Proglacial glacial outburst flood deposits comprise an extensive range of sediments driven by source proximity and the shape of the flood hydrograph (Clarke, 2003; Benn & Evans, 2010). However, at a meso- to small-scale, deposits are frequently characterised by complex facies associations and bounding surface geometries which reflect marked and rapid shifts in energy regime, sediment supply and turbulence (Maizels, 1992, 1993, 1997; Marren, 2005; Russell *et al.*, 2005; Duller *et al.*, 2008; Marren *et al.*, 2009). This meso- to small-scale architectural and sedimentological complexity is not apparent in the sequences at Lleiniog. Instead, Lithofacies A and B show comparatively steady longitudinal bedform development driven by stable helicoidal flows as the hydraulic regime / sediment budget adjusted to progressive channel widening and capture.

5.2 Development and preservation of large-scale sinusoidal bedforms

Large-scale sinusoidal bedforms with stoss- and lee-side preservation, including those described here, have been produced experimentally (Cheel, 1990) and recognised only rarely within the geological record (Fielding, 2006; Ito & Saito, 2006; Ito, 2010). Within a glacial context this includes subglacial drainage channels (Fisher *et al.*, 2003) and outburst floods (jökulhlaups) debouching either subaerially (Duller *et al.*, 2008) or onto subaqueous ice-contact fans (Lang & Winsemann, 2013). They have commonly been attributed to rapidly-aggrading stationary antidunes (Lang & Winsemann, 2010) that are supercritically climbing due to massive rates of sediment deposition under transitional dune to upper flow regimes (Cheel, 1990; Fielding, 2006).

The large-scale sinusoidal bedforms described here are slightly different because they were not stationary but migrating forwards leading to the development of their distinctive longitudinal form. These longitudinal bedforms highlight the importance of helicoidal processes within glacial meltwater systems (Brennand, 1994) although evidence is more commonly attributed to erosional processes that have sculpted the glacier bed (Menzies, 1989; Knight, 2009; Lesemann *et al.*, 2010a). Erosional bedforms will typically develop where fluid sediment concentrations are low and / or turbulence is high. This causes helicoidal vortices to become unstable, leading to lateral erosion and the generation of erosion surfaces (Duller *et al.*, 2008). By contrast, the semi-continuous to continuous sinusoidal bedforms at Lleiniog imply high and constant sediment concentrations, and stable helicoidal vortices that promoted net linear deposition (cf. Lang & Winsemann, 2013).

Helicoidal vortices commonly move in the direction of flow, while transverse flows (lower flow regime) which form at the interface with the underlying material, rotate backwards in the opposite direction to the overall fluid flow direction. This generates discrete zones of deposition and erosion with the absence of a 'counter-current' making helicoidal vortices much more efficient transporters of sediment. Such forms of flow can be depositional or erosional in-nature, or a combination of both, depending on the range of standard factors that control sediment deposition or entrainment within any moving fluid (Leeder, 2011). Bedforms observed at Lleiniog are generated by two co-existing mechanisms. Continuous sinusoidal bedforms with uniform thickness were generated by the fixing of helicoidal flows as the bedforms formed. This created a positive feedback within the adjacent vortices that produced stable vortices and equally stable (i.e. fixed) straight-crested bedforms. The truncated sinusoidal bedforms, by contrast, indicate occasional lateral movement of these vortices to produce sinuous helicoidal flows. These caused the lower limbs of several bedforms to be reshaped (i.e. thinned) by erosion and non-deposition with subsequent onlapping by beds from adjacent sinusoidal bedforms indicating a switch-back to stable vortices and bedforms. The dominantly continuous and in-phase stacking of the sinusoidal bedforms imply high sediment concentrations and rates of deposition (Allen, 1984).

Preservation of large-scale sinusoidal bedforms within the geological record is strongly influenced by turbulence which is partly a function of channel roughness (Kussin & Sommerfeld, 2002). Within subglacial drainage systems, channel roughness also includes the potential influence of ice-roof morphology (Walder, 1986). Flow-roof coupling would logically generate turbulence, causing helicoidal flow to become destabilised driving bedform erosion and sediment reworking. Alternatively, Fisher *et al.* (2003) have proposed flow-roof interaction coinciding with an abrupt drop in flow regime, could lead to the development of large-scale sinusoidal bedforms by the effect of ice-

Lee, J.R., Wakefield, O.J.W., Phillips, E. & Hughes, L. 2015. Sedimentary and structural evolution of a relict subglacial to subaerial drainage system and its hydrogeological implications: an example from Anglesey, north Wales, UK. *Quaternary Science Reviews* 109, 88-105. [ACCEPTED MANUSCRIPT]

moulding on flow and sediment. In the context of the Lleiniog sinusoidal bedforms, such a mechanism is not considered plausible. This is because the longitudinal (and vertical) development of the bedforms indicates that the flow regime was maintained during their formation - sinusoidal bedforms accreted during rapidly decelerating flow should climb with increasing steepness. Nevertheless, preservation of large-scale sinusoidal bedding does require turbulence to cease during or immediately after accretion (Fisher *et al.*, 2003; Fielding, 2006; Lang & Winsemann, 2010).

5.3 Recognition of subglacial meltwater deposits

A fundamental challenge facing glacial geologists is the confident recognition and interpretation of subglacial meltwater deposits. This is because of the critical role subglacial meltwater plays in regulating the dynamics of ice masses, ice-marginal behaviour and associated hydrogeological systems within subglacial, marginal and proglacial areas (Boulton & Hindmarsh, 1987; Piotrowski *et al.*, 2004, 2006; Evans & Hiemstra, 2005; Evans *et al.*, 2006; Robinson *et al.*, 2007; Boulton *et al.*, 2009; Bartholomew *et al.*, 2010). Put simply, subglacial meltwater deposits are the product of a hydrological regime that is not unique to subglacial environments, with similar regimes documented from a range of other sedimentary environments including intertidal (Cheel & Middleton, 1986), fluvial (Cheel, 1990, Røe, 1987; Alexander *et al.*, 2001) and channelised turbidity currents (Ito & Saito, 2006). Upper plane bed flow regimes have also been recognised within glacial meltwater systems including subglacial (this study; Brennand, 1994; Fisher *et al.*, 2003), englacial (Delaney, 2001, 2002) proglacial (Duller *et al.*, 2008) and subaqueous ice-contact environments (Russell & Arnott, 2003; Hornung *et al.*, 2007; Lang & Winsemann, 2013).

Upper flow regime bedform development within glacial environments is likely to be strongly influenced by all, or a combination of, flow confinement, elevated discharges and sediment budgets (Brennand, 1994; Duller *et al.*, 2008). These can relate to normal background flow conditions within confined channels (ice walled or incised into the bed), or constrained / unconstrained flow associated with high-magnitude glacier outburst flood events. Bedform preservation under such chaotic hydrological conditions is likely to be rare, requiring abrupt shut-down of the energy regime after formation to prevent bedforms from being reworked by turbulent eddies (Fisher *et al.*, 2003; Fielding, 2006; Lang & Winsemann, 2013). Their preservation within the geological record may be the exception rather than the rule (Fielding, 2006). Confident identification of subglacial meltwater sediments is therefore fraught with difficulty, especially when based simply upon hydrological parameters inferred from sedimentary evidence. Of critical importance is the recognition of other sediments and structures produced by subglacial processes and / or the geometric and sedimentary relationship to deposits of other deposits of subglacial origin (van der Wateren *et al.*, 2000). Indicators employed within this and other published studies (Mathers & Zalasiewicz, 1986; Piotrowski & Tulaczyk, 1999; Piotrowski *et al.*, 1999; Fisher *et al.*, 2003; Lesemann *et al.*, 2010b; Phillips & Lee, 2013) for the identification of subglacial meltwater scours, channels and sediments within the geological record are shown schematically in Figure 10. Key indicators include: (a) syn-sedimentary reverse and thrust faults produced by shear stresses transmitted into the sediment via the channels walls (subglacial bed or ice-walls); (b) subglacial traction till inter-bedded with meltwater deposits; (c) diamicton produced by the melt-out of debris-rich basal ice into a scour / channel and inter-bedded with meltwater deposits; (d) sediment bodies that extend beyond the lateral and vertical confines of the scour / channel implying lateral (ice-wall) constraint; (e)

Lee, J.R., Wakefield, O.J.W., Phillips, E. & Hughes, L. 2015. Sedimentary and structural evolution of a relict subglacial to subaerial drainage system and its hydrogeological implications: an example from Anglesey, north Wales, UK. *Quaternary Science Reviews* 109, 88-105. [ACCEPTED MANUSCRIPT]

sedimentary continuity (genetic and geometric) with subglacial scours, channels and deposits; (f) meltwater sedimentation progressively deformed (steepening and overturning) by subglacial deformation and possible interaction with subglacial till. Note the value of syn-sedimentary recumbent or conjugate folding within meltwater sediments is of more limited value because it can be produced by current-induced traction shearing of water-rich sediments.

5.4 Palaeoenvironmental Reconstruction

The glacial sequence exposed at Lleiniog contributes to a wider understanding of the glacial history of the Irish Sea Basin during the Late Weichselian (Devensian) glaciation (Ó Cofaigh & Evans, 2001a; Thomas & Chiverrell, 2007; Evans & Ó Cofaigh, 2008; Scourse *et al.*, 2009; McCarroll *et al.*, 2010; Phillips *et al.*, 2010; Clark *et al.*, 2012a; Chiverrell *et al.*, 2013). Erratic clasts from the basal and upper diamictos (Section 3; Greenly, 1919) are identical to those identified from Lithofacies B (Section 3 – Appendices 1 & 2) and derived from local- and far-travelled bedrock outcrops, and identify common sources for the entire Lleiniog sequence situated within and adjacent to the Irish Sea Basin (Phillips *et al.*, 2013). The simplest interpretation is that the basal diamicton was deposited during an initial southwards advance of Irish Sea Ice across Anglesey (Phillips *et al.*, 2013a) with a subsequent retreat and readvance across the island that deposited the upper diamicton associated with the overriding of the island by the Irish Sea Ice Stream (Thomas & Chiverrell, 2007; Phillips *et al.*, 2010; Clark *et al.*, 2012; Phillips & Hughes, 2014).

Following this model, the subglacial and proglacial outwash sequence at Lleiniog was deposited during the retreat of the ice margin that followed the initial advance across Anglesey. It records the development and subsequent collapse of a subglacial meltwater system that initially incised downwards into the subglacial bed probably as a series of physically-isolated meltwater incisions (Figure 11a). Thermal and mechanical erosion coupled with increased discharge presumably led to the merging and coalescence of individual drainage elements into progressively larger and more efficient, ice-contact, drainage channel(s) (Figure 11b). Sedimentation was driven by longitudinal bedform development under a transitional to upper flow regime with forward and vertical bedform migration driven by increasing and high sediment supply (Lithofacies A and B). The drainage system was then abandoned as a major outwash conduit with sedimentation driven by more ephemeral flow events. Further retreat of the ice margin to the north of the study area resulted in the deposition of the subaerial (proglacial) outwash sequence (Lithofacies C). Sedimentation occurred on a rapidly-aggrading braid-plane with phases of sheet-flow punctuated by episodes of lateral channel incision and aggradation within a diurnal, ablation-related, seasonal outwash system (Figure 11c). Loading and consolidation of the sediment pile is indicated by the presence of syn-sedimentary extensional faulting (Sites A and B) that variably truncate Lithofacies B and C. This includes a kettle-hole (Site C) formed by the melting of an isolated block of buried ice. Subsequent fault reactivation as hydrofracture systems provide clear evidence for variable and fluctuating groundwater conditions and periodic over-pressurisation of the local hydrological system leading to the rapid expulsion of water from the substrate (Phillips & Merritt 2008; Phillips *et al.*, 2013b). Hydrofracture systems have been widely recognised within subglacial to ice-marginal and proglacial settings (van der Meer *et al.*, 1999, 2009; Roberts *et al.*, 2009) and are important regulators of the hydrogeological system in glacial areas (Boulton *et al.*, 1993). The behaviour of glacial hydrogeological systems is known to vary

Lee, J.R., Wakefield, O.J.W., Phillips, E. & Hughes, L. 2015. Sedimentary and structural evolution of a relict subglacial to subaerial drainage system and its hydrogeological implications: an example from Anglesey, north Wales, UK. *Quaternary Science Reviews* 109, 88-105. [ACCEPTED MANUSCRIPT]

at a range of temporal and spatial scales (Robinson *et al.*, 2007). Changes are driven by standard processes that control groundwater systems, plus processes that operate within glacial environments including seasonal variations in temperature and meltwater flux, glacier surges and outburst floods (Robinson *et al.*, 2007). Several studies have demonstrated that such groundwater variability can exert a significant influence on subglacial and ice-marginal processes (Sharp, 1984; Krüger, 1994; Evans & Hiemstra, 2005) and this could have facilitated – at least locally, an ice-marginal readvance and deposition of the upper diamicton. This diamicton has been attributed elsewhere around the Irish Sea Basin with enhanced rates of basal sliding associated with the Late Weichselian Irish Sea Ice Stream (Ó Cofaigh & Evans, 2001a,b; Phillips *et al.*, 2010).

Conclusions

- Meltwater deposits at Lleiniog (Anglesey, North Wales) provide evidence for the temporal evolution of subglacial drainage (Lithofacies A and B) through to subaerial ice-marginal to proglacial drainage (Lithofacies C).
- Initial erosion of the upper surface of the basal diamicton (subglacial glacitectonite/till) by meltwater led to the incision of several deep, steep-sided, scours. Infilling of these scours by subglacial till and gravels (Lithofacies A) that dome-up beyond the confines of the channel are interpreted to signify a channelised subglacial origin with flow partitioned into discrete linear zones possibly confined by lateral ice walls. These meltwater channels are intermediate between N- and R-Channels in that both downward and upward incision occurred. One potential mechanism for the switch to upward incision into the overlying ice could be channel-armouring. Upstanding linear gravel ridges that infill these scours acted as nuclei for the growth of large-scale bedforms (upper flow regime) with lateral inter-fingering of the sediments (Lithofacies A) indicating bedform coalescence driven by channel expansion and merging with adjacent channels. Overlying sediments (Lithofacies B) comprise large-scale longitudinal bedforms with in-phase stacking of bedding producing sinusoidal-type bedding. Sinusoidal bedforms were produced within the transitional to upper flow regime under constant flow conditions but massive rates of sedimentation. Structural features provide evidence for traction-induced shearing of liquefied sediments (conjugate and recumbent folding) by sediment-laden flows, and modification of the channel walls by compressive shear stresses within the ice/bed (reverse faulting). Active channel use then switched to a more ephemeral discharge regime leading to channel abandonment indicating meltwater availability had ceased. This could be driven by seasonal changes in meltwater availability or re-routing of subglacial drainage via an alternate route. The subglacial sequence is overlain (conformably to unconformably) by sediments (Lithofacies C) interpreted as being deposited on a rapidly-aggrading subaerial (proglacial) braid-plane with a diurnal, ablation-related, seasonal discharge regime. Sedimentation was characterised by episodes of sheet flow punctuated by lateral channel incision and migration during lower flow stages.
- A wide range of meso-scale deformation structures including extensional faulting and hydrofractures truncate the sequence and formed during consolidation and loading of the sediment pile. Cross-cutting relationships between extensional faulting, hydrofractures and

Lee, J.R., Wakefield, O.J.W., Phillips, E. & Hughes, L. 2015. Sedimentary and structural evolution of a relict subglacial to subaerial drainage system and its hydrogeological implications: an example from Anglesey, north Wales, UK. *Quaternary Science Reviews* 109, 88-105. [ACCEPTED MANUSCRIPT]

hydrofracture fills, demonstrate marked fluctuations in groundwater levels and the cyclic development of an over-pressurised groundwater system. The importance of such systems is increasingly being recognised in subglacial, ice-marginal and proglacial areas because of its influence on glacier behaviour and subaerial processes.

- Positively identifying subglacial meltwater deposits is challenging. This is because in the first instance, their preservation-potential is limited due to other active meltwater and subglacial processes. Secondly, the range of facies generated by subglacial meltwater activity reflect a range of hydrological properties and processes that occur within other glacial and non-glacial setting. Of critical importance is the associated recognition of key features that are of subglacial origin including till and glaciectonic structures.

Acknowledgements

This research was funded by the Geology Landscape Wales project (Geology and Regional Geophysics Programme), British Geological Survey. Helen Burke, Richard Chiverrell, Jeremy Everest, Rhian Kendall, Felix Ng, James Scourse, Geoff Thomas and Amanda Williams are warmly thanked for their helpful discussions. Ann Rowan, Dave Evans and anonymous reviewer are acknowledged for their constructive comments on an earlier draft of this paper which have helped to improve and refine the manuscript. This paper is published with the permission of the Executive Director of the British Geological Survey (NERC).

References

- Alexander, J., Bridge, J.S., Cheel, R.J. & Leclair, S.F. 2001. Bedforms and associated sedimentary structures formed under supercritical water flows over aggrading sand beds. *Sedimentology* 48, 133-152.
- Allen, J.R.L. 1973. A classification of climbing-ripple cross-lamination. *Journal of the Geological Society* 129, 537-541.
- Allen, J.R.L. 1980. Sand waves: a model of origin and internal structure. *Sedimentary Geology* 26, 281-328.
- Alley, R.B., Clark, P.U., Huybrechts, P. & Joughin, I. 2005. Ice-Sheet and Sea-Level Changes. *Science* 310, 456-460.
- Bartholomew, I., Nienow, P., Mair, D., Hubbard, A., King, M.A. & Sole, A. 2010. Seasonal evolution of subglacial drainage and acceleration in a Greenland outlet glacier. *Nature Geoscience* 3, 408-411.
- Bell, R.E., Studinger, M., Shuman, C.A., Fahnestock, M.A. & Joughin, I., 2007. Large subglacial lakes in East Antarctica at the onset of fast-flowing ice streams. *Nature* 445, 904-907.
- Benediktsson, Í.Ö., Schomacker, A., Lokrantz, H. & Ingólfsson, Ó. The 1980 surge end moraine at Eyjabakkajökull, Iceland. A re-assessment of a classic glaciectonic locality. *Quaternary Science Reviews* 29, 484-506.
- Benn, D.I. & Prave, A.R. 2006. Subglacial and proglacial glaciectonic deformation in the Neoproterozoic Port Askaig Formation, Scotland. *Geomorphology* 75, 266-280.
- Benn, D. I. & Evans, D. J. A. 2010. *Glaciers and Glaciation* (Second Edition). Hodder Education, Abingdon. 802 pp.
- Bingham, R.G., Nienow, P.W., Shapr, M.J. & Boon, S. 2005. Subglacial drainage processes at a High Arctic polythermal valley glacier. *Journal of Glaciology* 51, 15-24.

- Lee, J.R., Wakefield, O.J.W., Phillips, E. & Hughes, L. 2015. Sedimentary and structural evolution of a relict subglacial to subaerial drainage system and its hydrogeological implications: an example from Anglesey, north Wales, UK. *Quaternary Science Reviews* 109, 88-105. [ACCEPTED MANUSCRIPT]
- Boulton, G.S., 1996. Theory of glacial erosion, transport and deposition as a consequence of subglacial sediment deformation. *Journal of Glaciology* 42, 43-62.
- Boulton, G.S. & Paul, M.A. 1976. The influence of genetic processes on some geotechnical properties of glacial tills. *Quarterly Journal of Engineering Geology* 9, 159-194.
- Boulton, G.S. & Hindmarsh, R.C.A., 1987. Sediment deformation beneath glaciers: Rheology and geological consequences. *Journal of Geophysical Research: Solid Earth* 92, 9059-9082.
- Boulton, G.S., Slot, T., Blessing, K., Glasbergen, P., Leijnse, T. & van Gijssel, K. 1993. Deep circulation of groundwater in overpressurised subglacial aquifers and its geological consequences. *Quaternary Science Reviews* 12, 739-745.
- Boulton, G.S., Hagdorn, M., Maillot, P.B. & Zatzepin, S. 2009. Drainage beneath ice sheets: groundwater-channel coupling, and the origin of esker systems from former ice sheets. *Quaternary Science Reviews* 28, 621-638.
- Bradwell, T., Stoker, M.S., Golledge, N.R., Wilson, C.K., Merritt, J.W., Long, D., Everest, J.D., Hestvik, O.B., Stevenson, A.G., Hubbard, A.L., Finlayson, A.G. & Mathers, H.E. 2008. The northern sector of the last British Ice Sheet: Maximum extent and demise. *Earth-Science Reviews* 88, 207-226.
- Brennand, T.A. 1994. Macroforms, large bedforms and rhythmic sedimentary sequences in subglacial eskers, south-central Ontario: implications for esker genesis and meltwater regime. *Sedimentary Geology* 91, 9-55.
- Brennand, T.A. & Sharpe, D.R. 1993. Ice-sheet dynamics and subglacial meltwater regime inferred from form and sedimentology of glaciofluvial systems: Victoria Island, District of Franklin, Northwest Territories. *Canadian Journal of Earth Sciences* 30, 928-944.
- Brennand, T.A. & Shaw, J. 1994. Tunnel channels and associated landforms, south-central Ontario: their implications for ice-sheet hydrology. *Canadian Journal of Earth Sciences* 31, 505-522.
- Burke, M.J., Brennand, T.A. & Perkins, A.J. 2012. Evolution of the subglacial hydrologic system beneath the rapidly decaying Cordilleran Ice Sheet caused by ice-dammed lake drainage: Implications for meltwater-induced ice acceleration. *Quaternary Science Reviews* 50, 125-140.
- Campbell, S. & Bowen, D. 1989. *The Quaternary of Wales*. Geological Conservation Review. 237 pp.
- Cant, D.J. & Walker, R.G. 1976. Development of braided-fluvial facies model for the Devonian Battery Point Sandstone, Québec. *Canadian Journal of Earth Sciences* 12, 102-119.
- Cheel, R.J. 1990. Horizontal laminatin and the sequence of bed phases and stratification under upper-flow-regime conditions. *Sedimentology* 37, 517-529.
- Chiverrell, R.C., Thrasher, I.M., Thomas, G.S.P., Lang, A., Scourse, J.D., van Landeghem, K.J.J., McCarroll, D., Clark, C.D., Cofaigh, C.Ó., Evans, D.J.A. & Ballantyne, C.K. 2013. Bayesian modelling the retreat of the Irish Sea Ice Stream. *Journal of Quaternary Science* 28, 200-209.
- Clark, C.D. & Meehan, R.T. 2001. Subglacial bedform geomorphology of the Irish Ice Sheet reveals major configuration changes during growth and decay. *Journal of Quaternary Science* 16, 483-496.
- Clark, C.D., Hughes, A.L.C., Greenwood, S.L., Jordan, C. & Sejrup, H.P. 2012. Pattern and timing of retreat of the last British-Irish Ice Sheet. *Quaternary Science Reviews* 44, 112-146.
- Clark, J., McCabe, A.M., Bowen, D.Q. & Clark, P.U. 2012. Response of the Irish Ice Sheet to abrupt climate change during the last deglaciation. *Quaternary Science Reviews* 35, 100-115.
- Clark, P.U. 1994. Unstable behavior of the Laurentide Ice Sheet over deforming sediment and its implications for climate change. *Quaternary Research* 41, 19-25.
- Clark, P.U. & Walder, J.S. 1994. Subglacial drainage, eskers, and deforming beds beneath the Laurentide and Eurasian ice sheets. *Geological Society of America Bulletin* 106, 304-314.
- Clarke, G.K., 2003. Hydraulics of subglacial outburst floods: new insights from the Spring-Hutter formulation. *Journal of Glaciology* 49, 299-313.

- Lee, J.R., Wakefield, O.J.W., Phillips, E. & Hughes, L. 2015. Sedimentary and structural evolution of a relict subglacial to subaerial drainage system and its hydrogeological implications: an example from Anglesey, north Wales, UK. *Quaternary Science Reviews* 109, 88-105. [ACCEPTED MANUSCRIPT]
- Dahl, R. 1965. Plastically sculptured detail forms on rock surface in northern Nordland, Norway. *Geografiska Annaler* 47, 83-140.
- Delaney, C. 2001. Morphology and sedimentology of the Rooskagh esker, County Roscommon. *Irish Journal of Earth Sciences*, 5-22.
- Delaney, C. 2002. Sedimentology of a glaciofluvial landsystem, Lough Ree area, Central Ireland: implications for ice margin characteristics during Devensian deglaciation. *Sedimentary Geology* 149, 111-126.
- Dowdeswell, J.A. & Siegert, M.J. 2003. The physiography of modern Antarctic subglacial lakes. *Global and Planetary Change* 35, 221-236.
- Duller, R. A., Mountney, N. P., Russell, A. J. & Cassidy, N. C. 2008. Architectural analysis of a volcanoclastic jökulhlaup deposit, southern Iceland: sedimentary evidence for supercritical flow. *Sedimentology* 55, 939-964.
- Ehlers, J. 1990. Reconstructing the dynamics of the north-west European Pleistocene ice sheets. *Quaternary Science Reviews* 9, 71-83.
- Evans, D. J.A. & Rea, B.R. 1999. Geomorphology and sedimentology of surging glaciers: a land-systems approach. *Annals of Glaciology* 28, 75-82.
- Evans, D.J.A. & Twigg, D.R. 2002. The active temperate glacial landsystem: A model based on Breicrossed d signamerkurjökull and Fjallsjökull, Iceland. *Quaternary Science Reviews* 21, 2143-2177.
- Evans, D.J.A. & Hiemstra, J.F. 2005. Till deposition by glacier submarginal, incremental thickening. *Earth Surface Processes and Landforms* 30, 1633-1662.
- Evans, D.J.A. & Ó Cofaigh, C. 2008. The sedimentology of the Late Pleistocene Bannow Till stratotype, County Wexford, southeast Ireland. *Proceedings of the Geologists' Association* 119, 329-338.
- Evans, D.J.A., Owen, L.A. & Roberts, D.H. 1995. Stratigraphy and sedimentology of Devensian (Dimlington Stadial) glacial deposits, east Yorkshire, England. *Journal of Quaternary Science* 10, 241-265.
- Evans, D.J.A., Clark, C.D. & Mitchell, W.A. 2005. The last British Ice Sheet: A review of the evidence utilised in the compilation of the Glacial Map of Britain. *Earth-Science Reviews* 70, 253-312.
- Evans, D.J.A., Phillips, E.R., Hiemstra, J.F. & Auton, C.A. 2006. Subglacial till: Formation, sedimentary characteristics and classification. *Earth-Science Reviews* 78, 115-176.
- Everest, J. & Bradwell, T. 2003. Buried glacier ice in southern Iceland and its wider significance. *Geomorphology* 52, 347-358.
- Eyles, N., McCabe, A., 1989. Glaciomarine facies within subglacial tunnel valleys: the sedimentary record of glacioisostatic downwarping in the Irish Sea Basin. *Sedimentology* 36, 431-448.
- Eyles, N., Doughty, M., Boyce, J.I., Mullins, H.T., Halfman, J.D. & Koseoglu, B. 2003. Acoustic architecture of glaciolacustrine sediments deformed during zonal stagnation of the Laurentide Ice Sheet; Mazinaw Lake, Ontario, Canada. *Sedimentary Geology* 157, 133-151.
- Fay, H. 2002. Formation of kettle holes following a glacial outburst flood (jökulhlaup), Skeidarársandur, southern Iceland. *The Extremes of the Extremes: Extraordinary Floods*, Int. Assoc. Hydrol. Sci. Publ 271, 205-210.
- Fielding, C.R. 2006. Upper flow regime sheets, lenses and scour fills: extending the range of architecture elements for fluvial sediment bodies. *Sedimentary Geology* 190, 227-240.
- Fisher, T.G., Taylor, L.D. & Jol, H.M. 2003. Boudier-gravel hummocks and wavy basal till contacts: products of subglacial meltwater flow beneath the Saginaw Lobe, south-central Michigan, USA. *Boreas* 32, 328-336.
- Flint, R.F., 1971. *Glacial and Quaternary Geology*. Wiley, 906 pp.
- Folk, R.L. 1976. Rollers and ripples in sand, streams and sky: rhythmic alteration of transverse and longitudinal vortices in three orders. *Sedimentology* 23, 649-668.
- Fowler, A. 1987. Sliding with cavity formation. *Journal of Glaciology* 33, 255-267.
- Fraser, G.S. 1993. Sedimentation in an interlobate outwash stream. *Sedimentary Geology* 83, 53-70.

- Lee, J.R., Wakefield, O.J.W., Phillips, E. & Hughes, L. 2015. Sedimentary and structural evolution of a relict subglacial to subaerial drainage system and its hydrogeological implications: an example from Anglesey, north Wales, UK. *Quaternary Science Reviews* 109, 88-105. [ACCEPTED MANUSCRIPT]
- Fürst, J.J., Goelzer, H. & Huybrechts, P. 2014. Ice-dynamic projects of the Greenland ice sheet in response to atmospheric and oceanic warming. *The Cryosphere Discuss* 8, 3851-3905.
- Goelzer, H., Huybrechts, P., Loutre, M.F., Goosse, H., Fichet, T. & Mouchet, A. 2011. Impact of Greenland and Antarctic ice sheet interactions on climate sensitivity. *Climate Dynamics* 37, 1005-1018.
- Greenly, E. 1919. *The Geology of Anglesey*, Memoirs of the Geological Survey of Great Britain. HMSO, London. 980 pp.
- Greenwood, S.L. & Clark, C.D. 2009. Reconstructing the last Irish Ice Sheet 1: changing flow geometries and ice flow dynamics deciphered from the glacial landform record. *Quaternary Science Reviews* 28, 3085-3100.
- Gustavson, T.C. & Boothroyd, J.C. 1987. A depositional model for outwash, sediment sources, and hydrologic characteristics, Malaspina Glacier, Alaska: A modern analog of the southeastern margin of the Laurentide Ice Sheet. *Geological Society of America Bulletin* 99, 187-200.
- Hallet, B. & Anderson, R. 1982. Detailed glacial geomorphology of a proglacial bedrock area at Castleguard Glacier, Alberta, Canada. *Zeitschrift für Gletscherkunde und Glazialgeologie* 16, 171-184.
- Ham, N.R. & Attig, J.W. 1996. Ice wastage and landscape evolution along the southern margin of the Laurentide Ice Sheet, north-central Wisconsin. *Boreas* 25, 171-186.
- Hambrey, M. 1984. Sedimentary processes and buried ice phenomena in the pro-glacial areas of Spitsbergen glaciers. *Journal of Glaciology* 30, 116-119.
- Hanna, E., Navarro, F.J., Pattyn, F., Domingues, C.M., Fettweis, X., Ivins, E.R., Nicholls, R.J., Ritz, C., Smith, B., Tulaczyk, S., Whitehouse, P.L. & Zwally, H.J. 2013. Ice-sheet mass balance and climate change. *Nature* 498, 51-59.
- Hart, J.K. 1995. Drumlin formation in Southern Anglesey and Arvon, Northwest Wales. *Journal of Quaternary Science* 10, 3-14.
- Helm, D.G. & Roberts, B. 1984. The Origin of late Devensian sands and gravels, southeast Anglesey, N. Wales. *Geological Journal* 19, 33-55.
- Hewitt, I.J., 2013. Seasonal changes in ice sheet motion due to melt water lubrication. *Earth and Planetary Science Letters* 371-372, 16-125.
- Hiemstra, J.F., Evans, D.J.A., Scourse, J.D., McCarroll, D., Furze, M.F.A. & Rhodes, E. 2006. New evidence for a grounded Irish Sea glaciation of the Isles of Scilly, UK. *Quaternary Science Reviews* 25, 299-309.
- Hodgkins, R. 1997. Glacier hydrology in Svalbard, Norwegian high arctic. *Quaternary Science Reviews* 16, 957-973.
- Hornung, J.J., Asprion, U. & Winsemann, J. 2007. Jet-efflux deposits of a subaqueous ice-contact fan, glacial Lake Rinteln, northwestern Germany. *Sedimentary Geology* 193, 167-192.
- Hubbard, A., Bradwell, T., Gollledge, N., Hall, A., Patton, H., Sugden, D., Cooper, R. & Stoker, M. 2009. Dynamic cycles, ice streams and their impact on the extent, chronology and deglaciation of the British-Irish ice sheet. *Quaternary Science Reviews* 28, 758-776.
- Ito, M. 2010. Are coarse-grained sediment waves formed as downstream-migrating antidunes? Insight from an early Pleistocene submarine canyon on the Boso Peninsula, Japan. *Sedimentary Geology* 226, 1-8.
- Iverson, N.R., Hanson, B., Hooke, R.L. & Jansson, P. 1995. Flow Mechanism of Glaciers on Soft Beds. *Science* 267, 80-81.
- Jopling, A.V. & Walker, R.G. 1968. Morphology and origin of ripple-drift cross-lamination, with example from the Pleistocene of Massachusetts. *Journal of Sedimentary Petrology* 38, 971-984.
- Kamb, B., Raymond, C., Harrison, W., Engelhardt, H., Echelmeyer, K., Humphrey, N., Brugman, M., Pfeffer, T. 1985. Glacier surge mechanism: 1982–1983 surge of Variegated Glacier, Alaska. *Science* 227, 469-479.

- Lee, J.R., Wakefield, O.J.W., Phillips, E. & Hughes, L. 2015. Sedimentary and structural evolution of a relict subglacial to subaerial drainage system and its hydrogeological implications: an example from Anglesey, north Wales, UK. *Quaternary Science Reviews* 109, 88-105. [ACCEPTED MANUSCRIPT]
- Kamb, B., 1987. Glacier surge mechanism based on linked cavity configuration of the basal water conduit system. *Journal of Geophysical Research: Solid Earth* 92, 9083-9100.
- Kelling, G. & Walton, E.K. 1957. Load-cast structures: their relationship to Upper-Surface Structures and their Mode of Formation. *Geological Magazine* 94, 481-490.
- Kjær, K.H., Larsen, E., van der Meer, J.J.M., Ingólfsson, Ó., Krüger, J., Örn Benediktsson, Í., Knudsen, C. G. & Schomacker, A. 2006. Subglacial decoupling at the sediment/bedrock interface: a new mechanism for rapid flowing ice. *Quaternary Science Reviews* 25, 2704-2712.
- King, M.A., Bingham, R.J., Moore, P., Whitehouse, P.L., Bentley, M.J. & Milne, G.A. 2012. Lower satellite-gravimetry estimates of Antarctic sea-level contribution. *Nature* 491, 586-589.
- Knight, J., McCarron, S. & McCabe, A.M. 1999. Landform modification by palaeo-ice streams in east central Ireland. *Annals of Glaciology* 28, 161-167.
- Kraus, M.J. & Middleton, L.T. 1987. Dissected paleotopography and base-level changes in a Triassic fluvial sequence. *Geology* 15, 18-21.
- Krüger, J. 1995. Origin, chronology and climatological significance of annual-moraine ridges at Myrdalsjökull, Iceland. *The Holocene* 5, 420-427.
- Krüger, J. 1997. Development of minor outwash fans at Kötlujökull, Iceland. *Quaternary Science Reviews* 16, 649-659.
- Kussin, J. & Sommerfeld, M. 2002. Experimental studies on particle behaviour and turbulence modification in horizontal channel flow with different wall roughness. *Experiments in Fluids* 33, 143-159.
- Lang, J. & Winsemann, J. 2013. Lateral and vertical facies relationships of bedforms deposited by aggrading supercritical flows: From cyclic steps to humpback dunes. *Sedimentary Geology* 296, 36-54.
- Langford, R. & Bracken, B. 1987. Medano Creek, Colorado - a model for upper-flow-regime fluvial deposition. *Journal of Sedimentary Research* 57, 863-870.
- Lee, J.R. & Phillips, E.R. 2008. Progressive soft sediment deformation within a subglacial shear zone—a hybrid mosaic-pervasive deformation model for Middle Pleistocene glaciotectionised sediments from eastern England. *Quaternary Science Reviews* 27, 1350-1362.
- Lee, J.R., Phillips, E., Booth, S.J., Rose, J., Jordan, H.M., Pawley, S.M., Warren, M., Lawley, R.S. 2013. A polyphase glaciectonic model for ice-marginal retreat and terminal moraine development: the Middle Pleistocene British Ice Sheet, north Norfolk, UK. *Proceedings of the Geologists' Association* 124, 753-777.
- Lian, O.B., Hicik, S.R. & Dreimanis, A. 2003. Laurentide and Cordilleran fast ice flow: some sedimentological evidence from Wisconsinian subglacial till and its substrate. *Boreas* 32, 102-113.
- Little, W.C. & Mayer, P.G. 1976. Stability of channel beds by armoring. *Journal of the Hydraulics Division* 102, 1647-1661.
- Lowe, D.R., 1975. Water escape structures in coarse-grained sediments. *Sedimentology* 22, 157-204.
- Lesemann, J., Piotrowski, J.A. & Wysota, W., 2010a. "Glacial curvilineations": New glacial landforms produced by longitudinal vortices in subglacial meltwater flows. *Geomorphology* 120, 153-161.
- Lesemann, J., Alsop, G.I. & Piotrowski, J.A. 2010b. Incremental subglacial meltwater sediment deposition and deformation with repeated ice-bed coupling: a case study from the Island of Funen, Denmark. *Quaternary Science Reviews* 29, 3212-3229.
- Lliboutry, L. 1968. General theory of subglacial cavitation and sliding of temperate glaciers. *Journal of Glaciology* 7, 21-58.
- MacAyeal, D. 1993. Binge/purge oscillations of the Laurentide ice sheet as a cause of the North Atlantic's Heinrich events. *Paleoceanography* 8, 775-784.
- Maizels, J. 1992. Boulder ring structures produced during Jökulhlaup flows. Origin and hydraulic significance. *Geografiska Annaler. Series A. Physical Geography*, 21-33.

- Lee, J.R., Wakefield, O.J.W., Phillips, E. & Hughes, L. 2015. Sedimentary and structural evolution of a relict subglacial to subaerial drainage system and its hydrogeological implications: an example from Anglesey, north Wales, UK. *Quaternary Science Reviews* 109, 88-105. [ACCEPTED MANUSCRIPT]
- Maizels, J. 1993. Lithofacies variations within sandur deposits: the role of runoff regime, flow dynamics and sediment supply characteristics. *Sedimentary Geology* 85, 299-325.
- Marren, P.M., 2005. Magnitude and frequency in proglacial rivers: a geomorphological and sedimentological perspective. *Earth-Science Reviews* 70, 203-251.
- Marren, P.M., Russell, A.J. & Rushmer, E.L., 2009. Sedimentology of a sandur formed by multiple jökulhlaups, Kverkfjöll, Iceland. *Sedimentary Geology* 213, 77-88.
- Mathers, S.J. & Zalasiewicz, J.A. 1986. A sedimentation pattern in Anglian marginal meltwater channels from Suffolk, England. *Sedimentology* 33, 559-573.
- McCarroll, D. & Rijdsdijk, K.F. 2003. Deformation styles as a key for interpreting glacial depositional environments. *Journal of Quaternary Science* 18, 473-489.
- McCarroll, D., Stone, J.O., Ballantyne, C.K., Scourse, J.D., Fifield, L.K., Evans, D.J.A. & Hiemstra, J.F. 2010. Exposure-age constraints on the extent, timing and rate of retreat of the last Irish Sea ice stream. *Quaternary Science Reviews* 29, 1844-1852.
- McCabe, P.J. & Jones, C.M. 1977. Formation of Reactivation Surfaces Within Superimposed Deltas and Bedforms. *Journal of Sedimentary Research* 47, 707-715.
- McDonald, B.C. & Banerjee, I. 1971. Sediments and bed forms on a braided outwash plain. *Canadian Journal of Earth Sciences* 8, 1282-1301.
- McMillan, A.A. & Merritt, J.W. 2012. A new Quaternary and Neogene Lithostratigraphical Framework for Great Britain and the Isle of Man. *Proceedings of the Geologists' Association* 123, 679-691.
- Menzies, J. 1989. Subglacial hydraulic conditions and their possible impact upon subglacial bed formation. *Sedimentary Geology* 62, 125-150.
- Miall, A.D. 1977. A review of the braided-river depositional environment. *Earth-Science Reviews* 13, 1-62.
- Miall, A.D. 1978. Lithofacies types and vertical profile models in braided river deposits: a summary. In Miall, A. D. (ed.): *Fluvial Sedimentology*, 597-604 pp. Canadian Society of Petroleum Geologists, Memoir 5.
- Miall, A.D. 1985. Architecture-elements analysis: A new method of facies analysis applied to fluvial deposits. *Earth-Science Reviews* 22, 261-308.
- Miall, A.D. 1988. Architectural elements and bounding surfaces in fluvial deposits: anatomy of the Kayenta formation (lower jurassic), Southwest Colorado. *Sedimentary Geology* 55, 233-262.
- Mulder, T. & Alexander, J. 2001. The physical character of subaqueous sedimentary density flows and their deposits. *Sedimentology* 48, 269-299.
- Nye, J.F. 1973. Water at the bed of a glacier. *International Association of Scientific Hydrogeologists Publication* 95, 189-194.
- Ó Cofaigh, C. 1996. Tunnel valley genesis. *Progress in Physical Geography* 20, 1-19.
- Ó Cofaigh, C. & Evans, D.J.A. 2001a. Sedimentary evidence for deforming bed conditions associated with a grounded Irish Sea glacier, southern Ireland. *Journal of Quaternary Science* 16, 435-454.
- Ó Cofaigh, C. & Evans, D.J.A. 2001b. Deforming bed conditions associated with a major ice stream of the last British Ice Sheet. *Geology* 29, 795-798
- Owen, G. 1996. Experimental soft-sediment deformation: structures formed by liquefaction of unconsolidated sands and some ancient examples. *Sedimentology* 43, 279-293.
- Owen, G. 2003. Load structures: gravity-driven sediment mobilization in the shallow subsurface. In: van Rensbergen, Hillis, R.R., Maltman, A.J. & Morley, C.K. (eds). *Subsurface Sediment Mobilisation*. Geological Society of London, Special Publication 216, 21-34.
- Pfeffer, W.T., Harper, J.T & O'Neel, S.O. 2008. Kinematic Constraints on Glacier Contributions to 21st-Century Sea-Level Rise. *Science* 321, 1340-1343.
- Phillips, E. & Merritt, J. 2008. Evidence for multiphase water-escape during rafting of shelly marine sediments at Clava, Inverness-shire, NE Scotland. *Quaternary Science Reviews* 27, 988-1011.

- Lee, J.R., Wakefield, O.J.W., Phillips, E. & Hughes, L. 2015. Sedimentary and structural evolution of a relict subglacial to subaerial drainage system and its hydrogeological implications: an example from Anglesey, north Wales, UK. *Quaternary Science Reviews* 109, 88-105. [ACCEPTED MANUSCRIPT]
- Phillips, E. & Lee, J.R. 2013. Development of a subglacial drainage system and its effect on glacitectonism within the polydeformed Middle Pleistocene (Anglian) glacial sequence of north Norfolk. *Proceedings of the Geologists' Association* 124, 855-875.
- Phillips, E. & Hughes, L. 2014. Hydrofracturing in response to the development of an overpressurised subglacial meltwater system during drumlin formation. *Proceedings of the Geologists' Association* 125, 296-311.
- Phillips, E., Everest, J. & Diaz-Doce, D. 2010. Bedrock controls on subglacial landform distribution and geomorphological processes: Evidence from the Late Devensian Irish Sea Ice Stream. *Sedimentary Geology* 232, 98-118.
- Phillips, E., Lee, J.R., Riding, J.B., Kendall, R. & Hughes, L. 2013a. Periglacial disruption and subsequent glacitectonic deformation of bedrock: an example from Anglesey, North Wales, UK. *Proceedings of the Geologists' Association* 124, 802-817.
- Phillips, E., Lipka, E. & van der Meer, J.J.M. 2013b. Micromorphological evidence of liquefaction and sediment deposition during basal sliding of glaciers. *Quaternary Science Reviews* 81, 114-137.
- Piotrowski, J.A. 1997. Subglacial hydrology in north-western Germany during the last glaciation: Groundwater flow, tunnel valleys and hydrological cycles. *Quaternary Science Reviews* 16, 169-185.
- Piotrowski, J.A., 1999. Channelized subglacial drainage under soft-bedded ice sheets: Evidence from small N-channels in Central European Lowland. *Geological Quarterly* 43, 153-162.
- Piotrowski, J.A., Tulaczyk, S., 1999. Subglacial conditions under the last ice sheet in northwest Germany: Ice-bed separation and enhanced basal sliding? *Quaternary Science Reviews* 18, 737-751.
- Piotrowski, J.A., Geletneky, J., Vater, R., 1999. Soft-bedded subglacial meltwater channel from the Welzow-Sud open-cast lignite mine, Lower Lusatia, eastern Germany. *Boreas* 28, 363-374.
- Piotrowski, J.A., Larsen, N.K. & Junge, F.W. 2004. Reflections on soft subglacial beds as a mosaic of deforming and stable spots. *Quaternary Science Reviews* 23, 993-1000.
- Piotrowski, J.A., Larsen, N.K., Menzies, J. & Wysota, W. 2006. Formation of subglacial till under transient bed conditions: Deposition, deformation, and basal decoupling under a Weichselian ice sheet lobe, central Poland. *Sedimentology* 53, 83-106.
- Ramsay, J.G. 1962. The Geometry of Conjugate Fold Systems. *Geological Magazine* 9, 516-526.
- Rijsdijk, K.F., Warren, W.P. & van der Meer, J.J.M. 2010. The glacial sequence of Killiney, SE Iceland: terrestrial deglaciation and polyphase glacitectonic deformation. *Quaternary Science Reviews* 19, 696-719.
- Rippin, D., Willis, I., Arnold, N., Hodson, A., Moore, J., Kohler, J. & Björnsson, H. 2003. Changes in geometry and subglacial drainage of Midre Lovénbreen, Svalbard, determined from digital elevation models. *Earth Surface Processes and Landforms* 28, 273-298.
- Robel, A.A., DeGiuli, E., Schoof, C., Tziperman, E. 2013. Dynamics of ice stream temporal variability: Modes, scales, and hysteresis. *Journal of Geophysical Research: Earth Surface* 118, 925-936.
- Roberts, D.H., Dackombe, R.V. & Thomas, G.S.P. 2007. Palaeo-ice streaming in the central sector of the British-Irish Ice Sheet during the Last Glacial Maximum: evidence from the northern Irish Sea Basin. *Boreas* 36, 115-129.
- Roberts, D.H. 2009. Ice marginal dynamics during surge activity, Kuannersuit Glacier, Disko Island, West Greenland. *Quaternary Science Reviews* 29, 209-222.
- Robinson, Z.P., Fairchild, I.J. & Russell, A.J. 2008. Hydrogeological implications of glacial landscape evolution at Skeiðarársandur, SE Iceland. *Geomorphology* 97, 218-236.
- Røe, S.-L. 1987. Cross-strata and bedforms of probable transitional dune to upper-stage plane-bed origin from a Late Precambrian fluvial sandstone, northern Norway. *Sedimentology* 34, 89-101.

- Lee, J.R., Wakefield, O.J.W., Phillips, E. & Hughes, L. 2015. Sedimentary and structural evolution of a relict subglacial to subaerial drainage system and its hydrogeological implications: an example from Anglesey, north Wales, UK. *Quaternary Science Reviews* 109, 88-105. [ACCEPTED MANUSCRIPT]
- Røe, S.-L. & Hermansen, M. 2006. New aspects of deformed cross-strata in fluvial sandstones: Examples from Neoproterozoic formations in northern Norway. *Sedimentary Geology* 186, 283-293.
- Röthlisberger, H. 1972. Water pressure in intra- and subglacial channels. *Journal of Glaciology* 11, 177-203.
- Russell, A.J., Knudsen, Ó., Fay, H., Marren, P.M., Heinz, J. & Tronicke, J. 2001. Morphology and sedimentology of a giant supraglacial, ice-walled, jökulhlaup channel, Skeiðarárjökull, Iceland: implications for esker genesis. *Global and Planetary Change* 28, 193-216.
- Russell, A.J., Fay, H., Marren, P.M., Tweed, F.S., Knudsen, Ó., 2005. Icelandic jökulhlaup impacts, In: Caseldine, C.J., Russell, A.J., Hardardottir, J., Knudsen, Ó. (Eds.), *Iceland: Modern Processes and Past Environments*. Elsevier, Amsterdam, pp. 153-203.
- Russell, H.A.J. & Arnott, R.W.C. 2003. Hydraulic-jump and hyperconcentrated-flow deposits of a glacial subaqueous fan: Oak Ridges Moraine, Southern Ontario, Canada. *Journal of Sedimentary Research* 73, 887-905.
- Rust, B.R. 1972a. Pebble orientation in fluvial sediments. *Journal of Sedimentary Petrology* 42, 384-388.
- Rust, B.R. 1972b. Structure and process in a braided river. *Sedimentology* 18, 221-245.
- Scourse, J.D., Haapaniemi, A.I., Colmenero-Hidalgo, E., Peck, V.L., Hall, I.R., Austin, W.E.N., Knutz, P.C. & Zahn, R. 2009. Growth, dynamics and deglaciation of the last British-Irish ice sheet: the deep-sea ice-rafted detritus record. *Quaternary Science Reviews* 28, 3066-3084.
- Sharp, M.J. 1984. Annual moraine ridges at Skalfellsjökull, south-east Iceland. *Journal of Glaciology* 6, 837-843.
- Sharp, M.J., Gemmell, J. C. & Tison, J.L. 1989. Structure and stability of the former subglacial drainage system of the Glacier de Tsanfleuron, Switzerland. *Earth Surface Processes and Landforms* 14, 119-134.
- Sherpherd, A. & Wingham, D. 2007. Recent sea-level contribution of the Antarctic and Greenland Ice Sheets. *Science* 315, 1529-1532.
- Shreve, R.L. 1972. Movement of water in glaciers. *Journal of Glaciology* 11, 205-214.
- Shreve, R.L. 1985. Esker characteristics in terms of glacier physics, Katahdin esker system, Maine. *Geological Society of America Bulletin* 96, 639-646.
- Smith, B.E., Fricker, H.A., Joughin, I.R. & Tulaczyk, S. 2009. An inventory of active subglacial lakes in Antarctica detected by ICESat (2003-2008). *Journal of Glaciology* 55, 573.
- Stokes, C.R., Clark, C.D., Lian, O.B., Tulaczyk, S., 2007. Ice stream sticky spots: A review of their identification and influence beneath contemporary and palaeo-ice streams. *Earth Science Reviews* 81, 217-279.
- Stone, P. 2012. The demise of the Iapetus Ocean as recorded in the rocks of southern Scotland. *Journal of the Open University Geological Society* 33, 29-36.
- Stone, P., Millward, D., Young, B., Merritt, J.W., Clarke, S., McCormac, M. & Lawrence, D. 2010. Northern England (British Regional Geology). 294 pp. British Geological Survey, Nottingham, UK.
- Synge, F., 1964. The Glacial Succession in West Caernarvonshire. *Proceedings of the Geologists' Association*, 75: 431-444.
- Sundal, A.V., Shepherd, A., Nienow, P., Hanna, E., Palmer, S. & Huybrechts, P. 2011. Melt-induced speed-up of Greenland ice sheet offset by efficient subglacial drainage. *Nature* 469, 521-524.
- Thomas, G.S.P. & Chiverrell, R.C. 2007. Structural and depositional evidence for repeated ice-marginal oscillation along the eastern margin of the Late Devensian Irish Sea Ice Stream. *Quaternary Science Reviews* 26, 2375-2405.
- Thomas, G.S.P. & Montague, E. 1997. The morphology, stratigraphy and sedimentology of the Carstairs esker, Scotland, U.K. *Quaternary Science Reviews* 16, 661-674.

- Lee, J.R., Wakefield, O.J.W., Phillips, E. & Hughes, L. 2015. Sedimentary and structural evolution of a relict subglacial to subaerial drainage system and its hydrogeological implications: an example from Anglesey, north Wales, UK. *Quaternary Science Reviews* 109, 88-105. [ACCEPTED MANUSCRIPT]
- Tulaczyk, S., Kamb, W.B., Engelhardt, H.F. 2000. Basal mechanics of Ice Stream B, west Antarctica: 1. Till mechanics. *Journal of Geophysical Research: Solid Earth* 105, 463-481.
- Tunbridge, I.P. 1981. Sandy high-energy flood sedimentation—some criteria for recognition, with an example from the Devonian of SW England. *Sedimentary Geology* 28, 79-95.
- van der Meer, J.J.M., Kjær, K.H. and Krüger, J. 1999. Subglacial water-escape structures and till structures, Sléttjökull, Iceland. *Journal of Quaternary Science*, 14: 191-205.
- van der Meer, J.J.M., Kjær, K.H., Krüger, J., Rabassa, J. & Kilfeather, A.A. 2009. Under pressure: clastic dykes in glacial settings. *Quaternary Science Reviews* 28, 708-720.
- van der Wateren, F.M., Kluiving, S.J. & Bartek, L.R., 2000. Kinematic indicators of subglacial shearing, In: Maltman, A.J., Hubbard, B., Hambrey, M.J. (Eds.), *Deformation of Glacial Materials*. Geological Society Special Publication No. 176, London, pp. 259-278.
- van Landeghem, K.J.J., Wheeler, A.J. & Mitchell, N.C. 2009. Seafloor evidence for palaeo-ice streaming and calving of the grounded Irish Sea Ice Stream: Implications for the interpretation of its final deglaciation phase. *Boreas* 38, 119-131.
- Walder, J.S. 1986. Hydraulics of subglacial cavities. *Journal of Glaciology* 32, 439-445.
- Walder, J.S. 2010. Röthlisberger channel theory: its origins and consequences. *Journal of Glaciology* 56, 1079-1086.
- Walsh, P.T., Butterworth, M.A. & Wright, K. 1982. The palynology and provenance of the coal fragments contained in the late-Pleistocene Lleiniog gravels of Anglesey, North Wales. *Geological Journal* 17, 23-30.
- Warren, W.P. & Ashley, G.M. 1994. Origins of the ice-contact stratified ridges (eskers) of Ireland. *Journal of Sedimentary Research* 64, 433-449.
- Williams, A.J. 2003. The sedimentology of Late Devensian glacial deposits in Anglesey, north-west Wales. Unpublished PhD Thesis, University of Liverpool.
- Wingfield, R. 1990. The origin of major incisions within the Pleistocene deposits of the North Sea. *Marine Geology* 91, 31-52.
- Zwally, H.J., Giovinetto, M.B., Li, J., Cornejo, H.G., Beckley, M.A., Brenner, A.C., Saba, J. & Yi, D. 2005. Mass changes of the Greenland and Antarctic ice sheets and sea-level rise: 1992-2002. *Journal of Glaciology* 51, 509-527.

Figure & Appendix Captions

Figure 1. Maps showing the location and context of the study site. **(a)** Map of eastern Anglesey showing the bedrock and Quaternary geology of the study area (British Geological Survey, unpublished data) and sites referred to within the text. **(b)** Map and NEXTMAP Digital Surface Model of Anglesey and northwest Wales showing the study site and ice sheet and glacier configuration during the Late Devensian (after Thomas and Chiverrell, 2007 and Phillips et al., 2010). **(c)** Map of the Britain and adjacent offshore areas showing the proximity of Anglesey relative to the Late Devensian ice limit and Irish Sea Ice Stream (after Phillips et al., 2010). Abbreviations: IOM – Isle of Man, LB – Liverpool Bay, LD – Lake District, COF – Cairnsmore of Fleet, CD – Criffel-Dalbeattie plutons.

Figure 2. Cross-section of the coastal exposures between Beaumaris and Trwyn y Penrhyn showing the geometry of the main Quaternary stratigraphic units.

Figure 3. (a) Mapped foreshore outcrop of Lithofacies A at Lleiniog showing the spatial distribution of dune ridges and trough areas, palaeocurrent measurements and reactivation surfaces (modified from Helm and Roberts, 1984). Vertical and horizontal scale according to UK National Grid – each grid square represents 10 m². **(b)** Cross-section z1-z2 through Lithofacies A on the foreshore at Lleiniog showing the geometric relationship between the lithofacies and the basal diamicton. **(c)** Cross-section y1-y2 on the Lleiniog foreshore showing the. Lithofacies Abbreviations: Dmm – diamicton, matrix-supported, massive; Dms – diamicton, matrix-supported, faintly-stratified; Gmm – gravel, matrix-supported, massive; Gcm – gravel, clast-supported, massive; Sm – sand, massive; Sh – sand – plane-bedded; St – sand, trough cross-bedded; Sr – sands, ripples; ---(r) – rip-up clasts composed of diamicton; --- (i) – crude imbrication; --- (l) – load structures; --- (fu) – fining-upwards.

Figure 4. (a) Photograph (facing north-northeast) showing sets of inter-fingering cross-bedding forests (Lithofacies A) derived from coalescing ridges [Photo: J. Lee]. **(b)** Large-scale sand and gravel bedforms (Lithofacies B) showing continuous parallel to sub-parallel bedding surfaces forming a series of ridges and troughs between 140-155m (see Figure 5) [Photo: J. Lee]. **(c)** Photograph (facing northwest) of clast-supported gravel (Lithofacies B) with bedding-parallel aligned elongate clasts at 117 m (see Figure 5) [Photo: J. Lee]. **(d)** Large-scale undulatory sandy bedforms (Lithofacies B) with bounding surfaces defining separate bedding-sets, note the hydrofracture system (blue) utilising pre-existing normal (extensional) faulting which extends upwards into the basal beds of Lithofacies C1 (facing northwest; 143m in Figure 5). **(e)** Large-scale undulatory bedforms (Lithofacies B) composed of sand and gravel and coarse sand between 213-227m (facing west, see Figure 5) [Photo: J. Lee]. **(f)** Thin mud drapes between sand ripples (facing northwest, at 2m Figure 5) [Photo: J. Everest]. **(g)** Coal fragments deposited on the inter-fingering foresets of Type 2 sinusoidal bedforms – facing northwest, at 8m (see Figure 5) [Photo: J. Lee]. **(h)** Conjugate folding developed within Lithofacies B underlying undeformed bedding (facing west, at 166m Figure 5) [Photo: E. Phillips]. **(i)** Small reverse fault within Lithofacies B at 84m (Figure 4) inclined towards the northwest – the white colouration is surface salt precipitation [Photo: J. Lee]. **(j)** Photograph showing Lithofacies C gravels resting conformably upon sands (Lithofacies B); note the large flame-structure produced by the loading of the sandy unit by the upper gravels (facing west, at 118m on Figure 5) [Photo: J. Lee]. **(k)** Erosional lower boundary of Lithofacies C forming the southern edge of an incised channel (facing west, 120m on Figure 5) [Photo: J. Lee]. **(l)** Irregular basal erosional surface (red) of Lithofacies C and additional major (yellow) and minor (orange) bounding surfaces (facing southwest, 100-113m on Figure 5) [Photo: J. Lee].

Figure 5. Cross-section of the cliff section from Lleiniog (NW) towards Tre-castell (SE) showing the sedimentology, structure and geometric relationship between the Lithofacies B, C and the overlying Irish Sea Diamicton (IBD). The location of palaeocurrent sample points are indicated with reference to Figure 5.

Figure 6. Palaeocurrent and structural measurements from the coastal cliff sections at Lleiniog – the location of sample points can be seen in Figure 3. **(a)** Equal-area lower hemisphere stereographic projection (Schmidt) of the dip angle and azimuth of thrusts and reverse faults plotted as great circles and poles to planes. **(b)** Lithofacies C palaeocurrents.

Lee, J.R., Wakefield, O.J.W., Phillips, E. & Hughes, L. 2015. Sedimentary and structural evolution of a relict subglacial to subaerial drainage system and its hydrogeological implications: an example from Anglesey, north Wales, UK. *Quaternary Science Reviews* 109, 88-105. [ACCEPTED MANUSCRIPT]

Figure 7. (a) Sand-filled fracture truncating Lithofacies B at Site A (4m, Figure 5). (b) Complex fracture sets (BF1-3) at Site B (30 m, Figure 3) showing evidence of normal faulting and hydrofracturing – the different blue-shaded fracture annotations relate to different cross-cutting stages of fracture development. (c) Detailed structural diagram showing the development of successive stages (CF1-CF3) of extensional fault development between 70-80m (Figure 5).

Figure 8. Schematic model showing the development of Lithofacies A. (a) Focused erosion of the subglacial bed (Basal Diamicton) creating deep scours. (b) Partial infill of the scour with basal lag (gravel and rip-up clasts), subglacial till and channel armouring (upper gravel) promoting upward meltwater incision into the ice. (c) Lateral widening of the ice-walled channel. (d) Confining ice walls enabling the vertical and lateral accretion of the gravels beyond the confines of the original scour - gravels cores subsequently acted as nuclei for sand deposition.

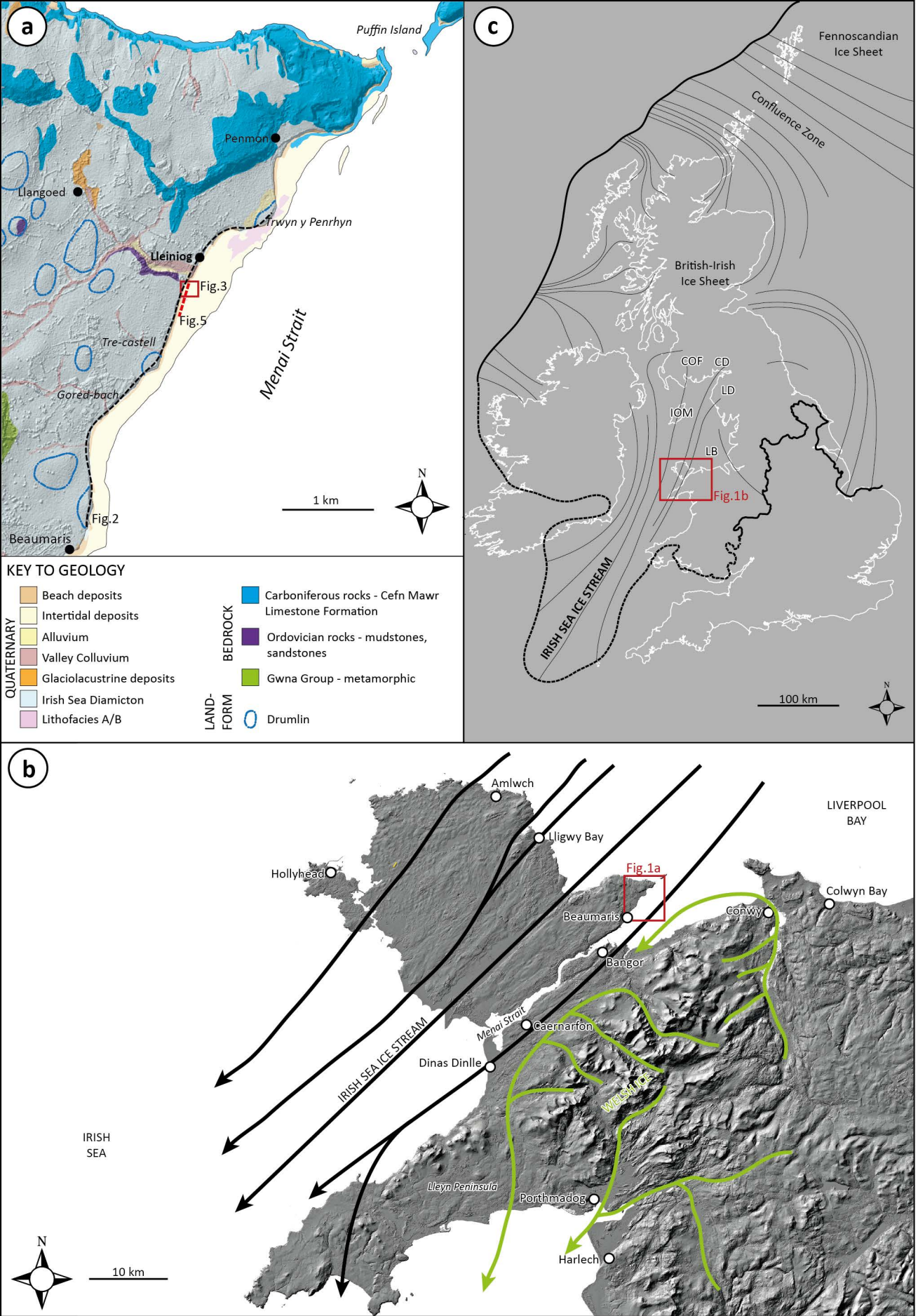
Figure 9. A series of three schematic block models showing the evolution of Lithofacies A-C. (a) Subglacial accretion of Lithofacies A which crops-out on the foreshore at Lleiniog showing the development of R-Channels which acted as nuclei for the development of longitudinal ridges with wash-out of the ridge crests to form the flank deposits. (b) Subglacial development of sinusoidal bedforms (Lithofacies B) by relatively stable helicoidal vortices. (c) Infilling of the substrate during a phase of subaerial (proglacial) braid-plain sedimentation (Lithofacies C). Note that the contact between Lithofacies A and B was not observed and is shown simply on the diagram as a straight line – this does not mean that the contact was horizontal.

Figure 10. Criteria to identify subglacial meltwater deposits including associations of meltwater scours / channels / deposits with subglacial till and debris derived from melt-out of debris-rich basal ice, reverse and thrust faults, vertically and laterally extending sediment bodies and sedimentary continuity. Note that the application of multiple criteria will improve confidence of interpretation.

Figure 11. Schematic models showing the evolution of palaeogeography and sediment facies variability (temporal and spatial) during the deposition of the Late Devensian sequence at Lleiniog. (a) Subglacial meltwater incision of the surface of the Basal Diamicton and development of focused scours (subglacial channels) and accretion of Lithofacies. (b) Coalescence and enlargement of subglacial channels and deposition of large-scale sinusoidal bedforms (Lithofacies B); traction shearing of sediments and channel morphology modification by the application of compressive stresses. (c) Retreat of the ice margin and subaerial (proglacial) deposition of outwash sands and gravels (Lithofacies C) as sheet and channelised flow; localised development of kettle structure representing the melting of stranded ice blocks, and loading and dewatering of the underlying sediment pile under fluctuating groundwater conditions.

Appendix 1. Summary of the petrology of sand to fine-gravel sized sediments within the glacial outwash sequence exposed in the coastal cliff section at Lleiniog, Anglesey, North Wales.

Appendix 2. Summary of the petrology of pebble to cobble sized clasts contained within Lithofacies B, Lleiniog, Anglesey, North Wales.



NEXTMap Britain elevation data from Intermap Technologies.

FIGURE 1

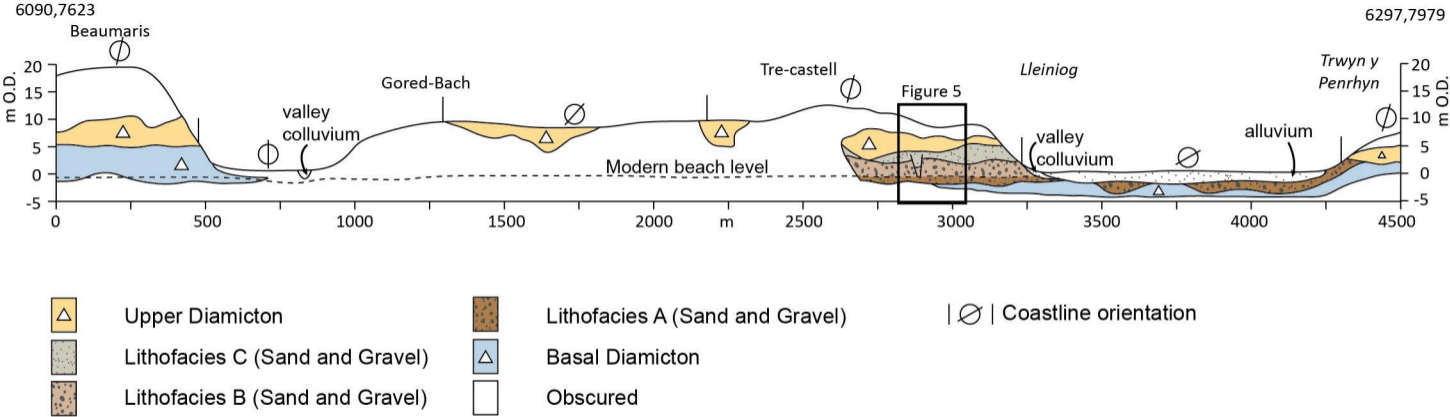
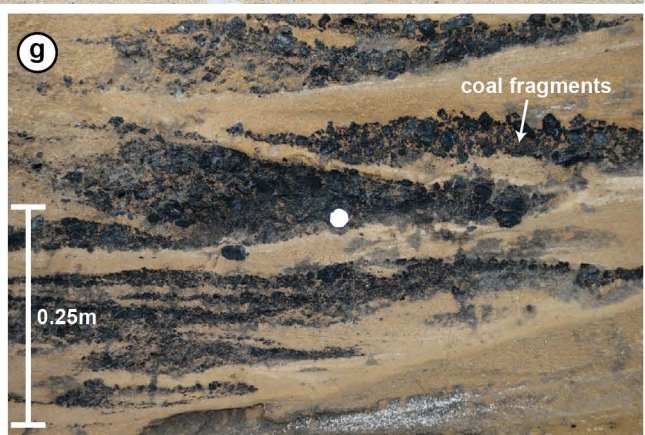
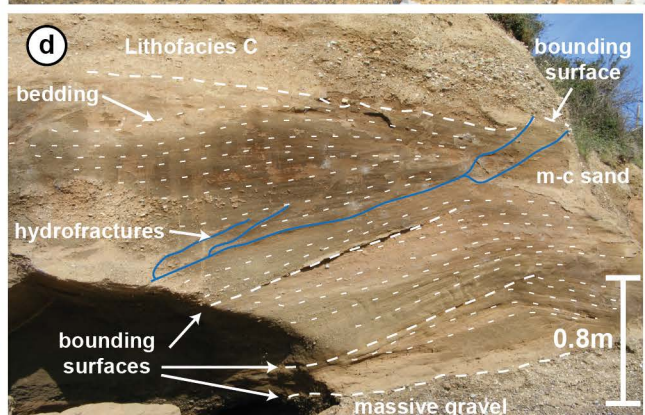
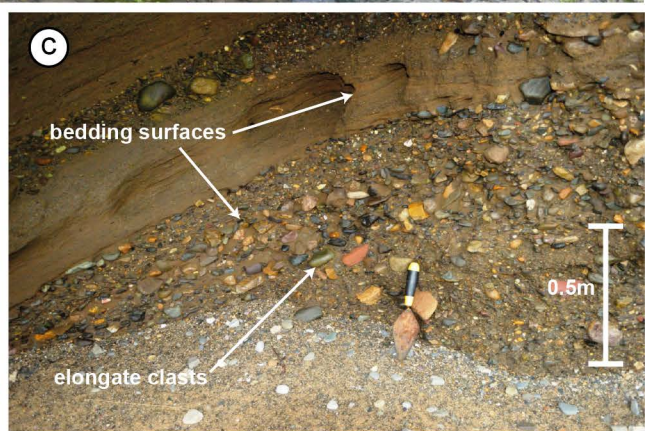


Figure 2



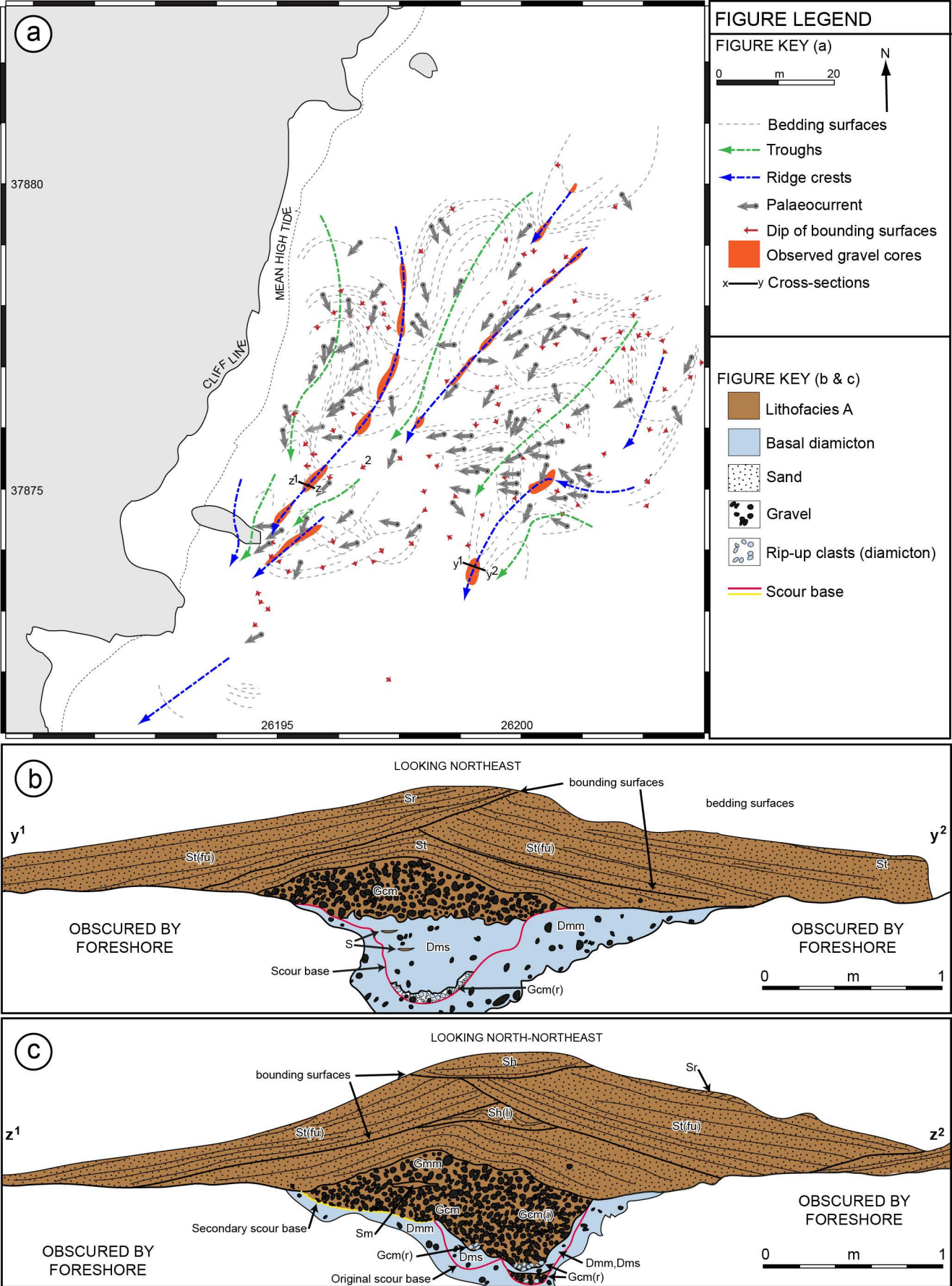
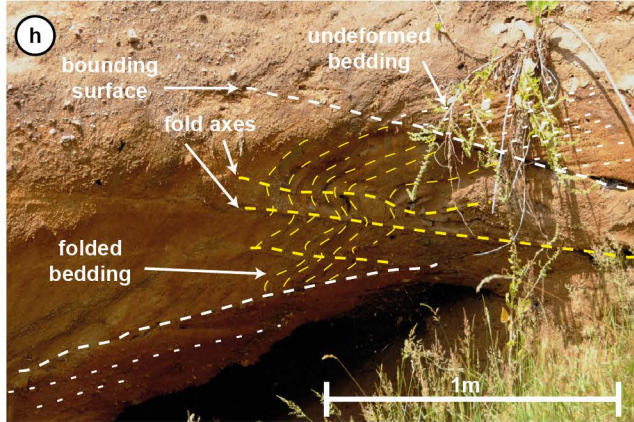
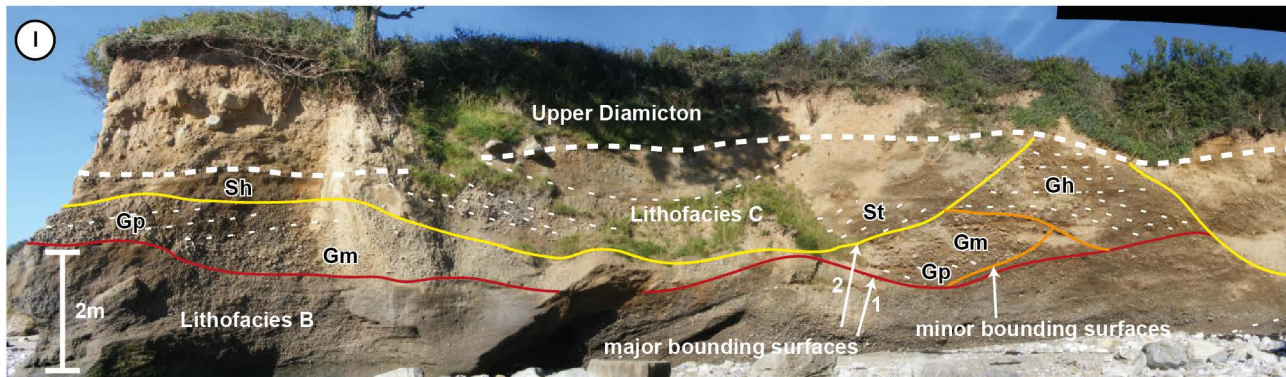
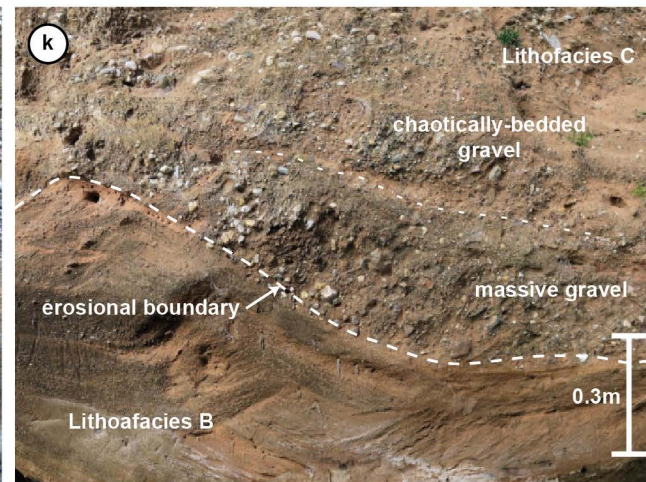
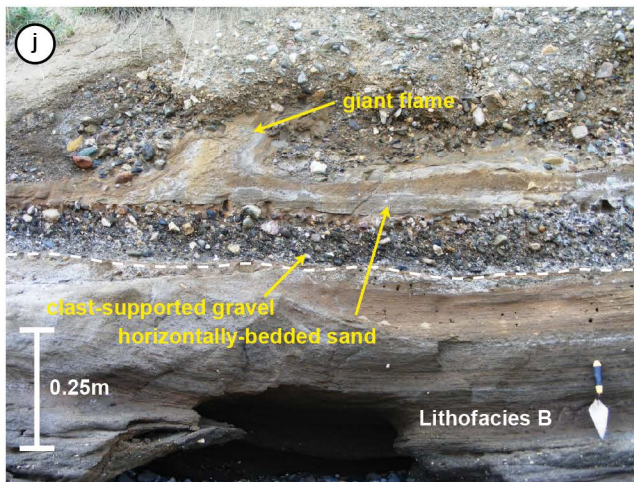


FIGURE 3



(i)



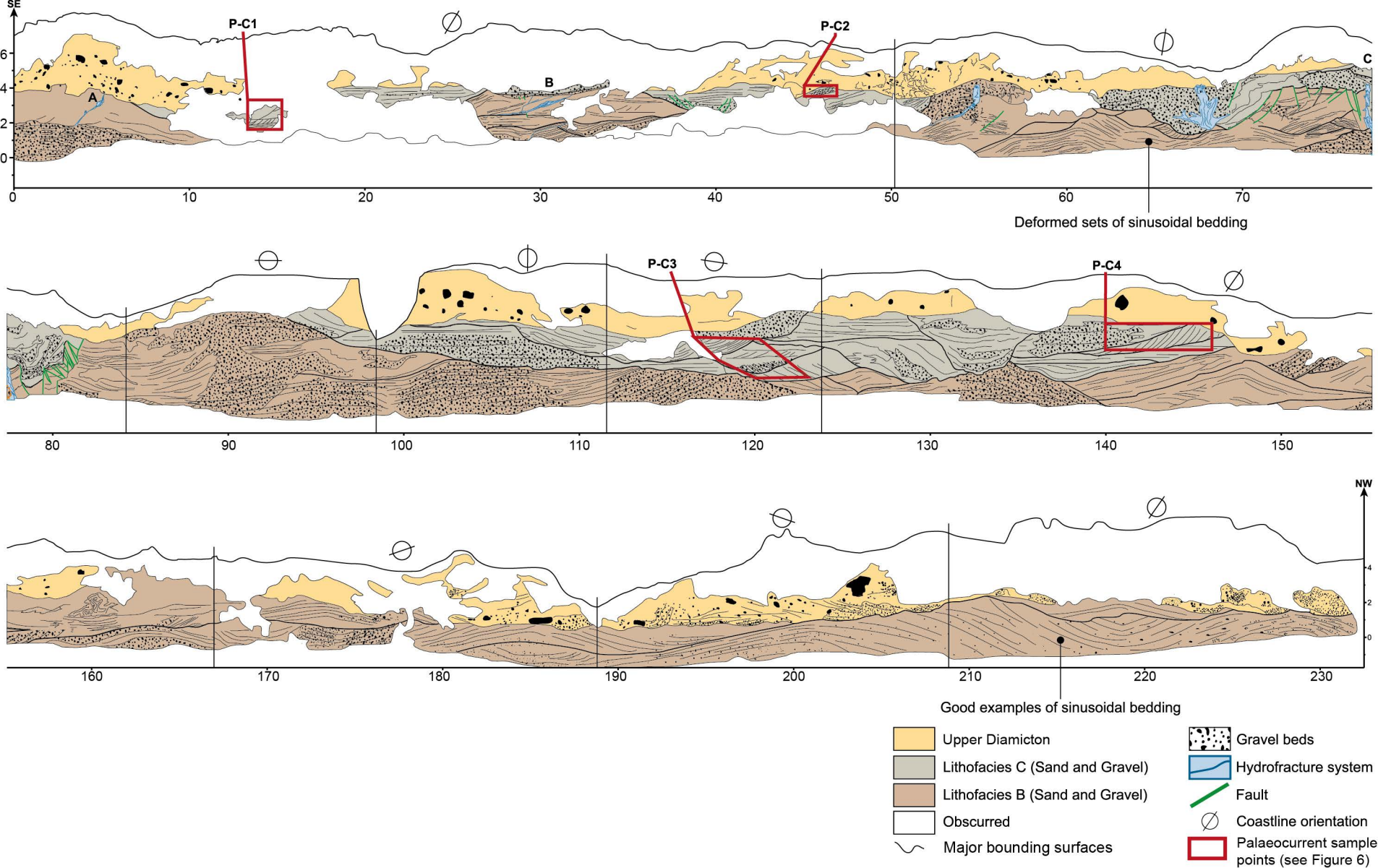
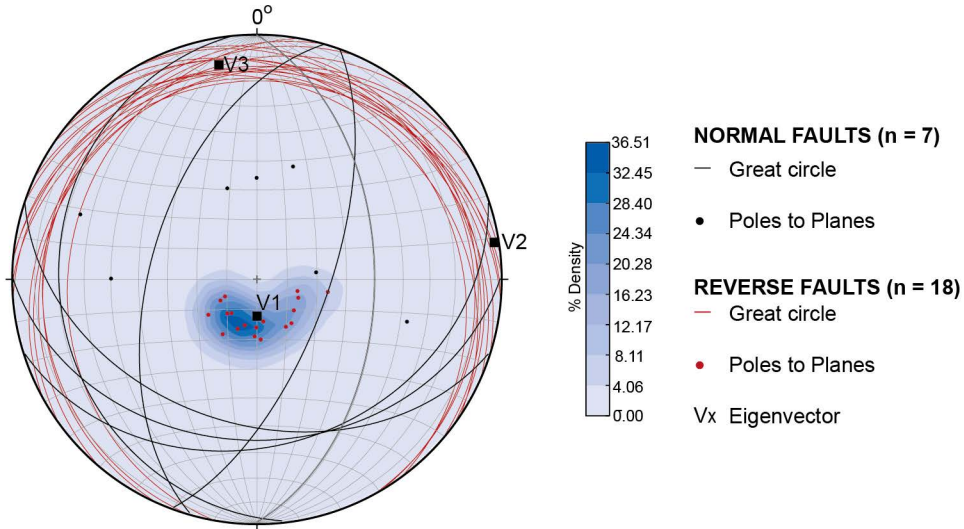


Figure 5

a)



b)

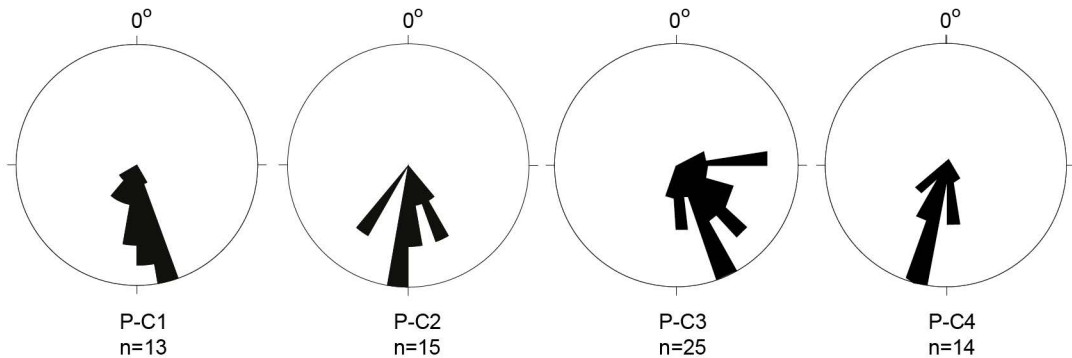


Figure 6

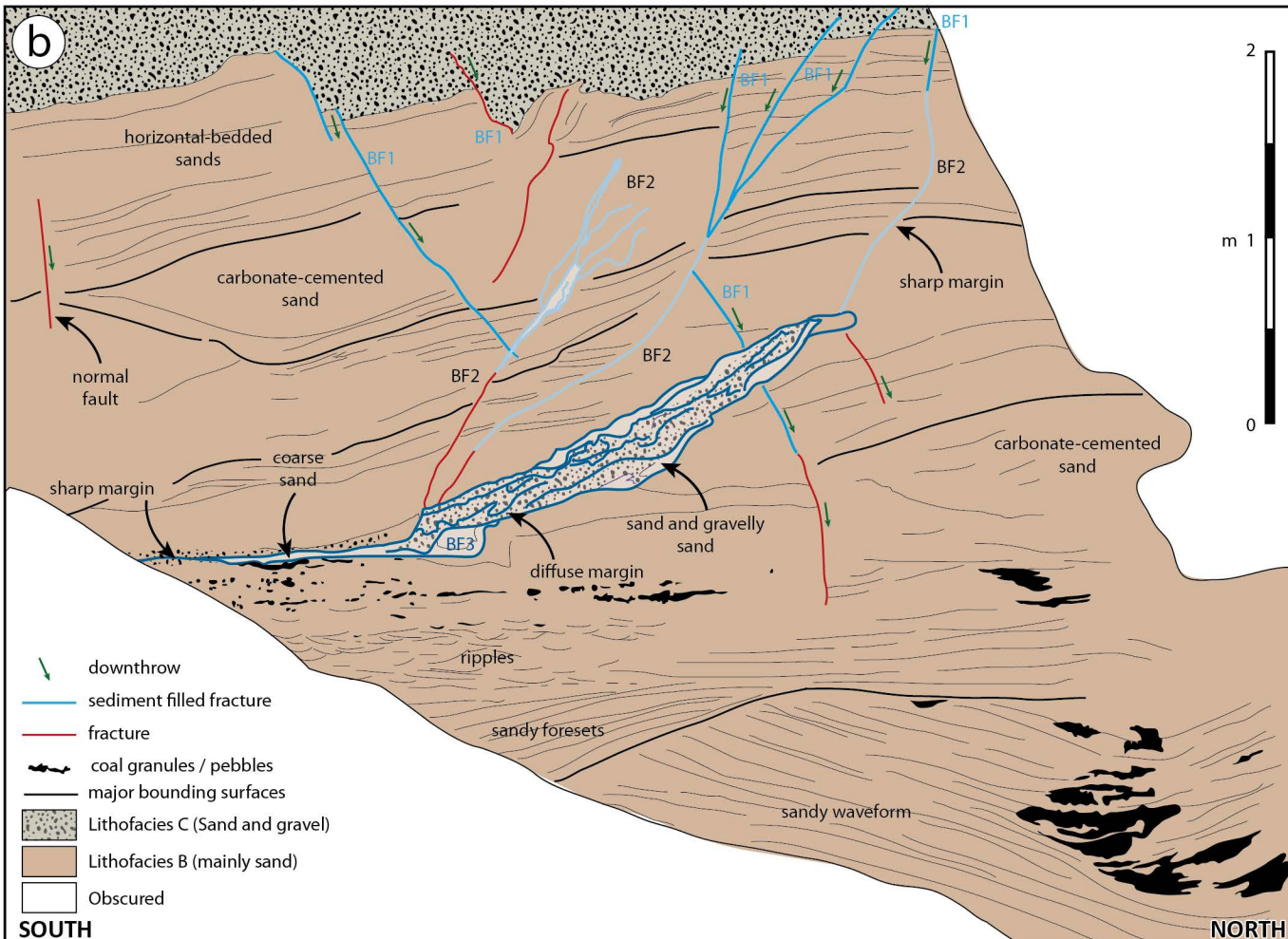
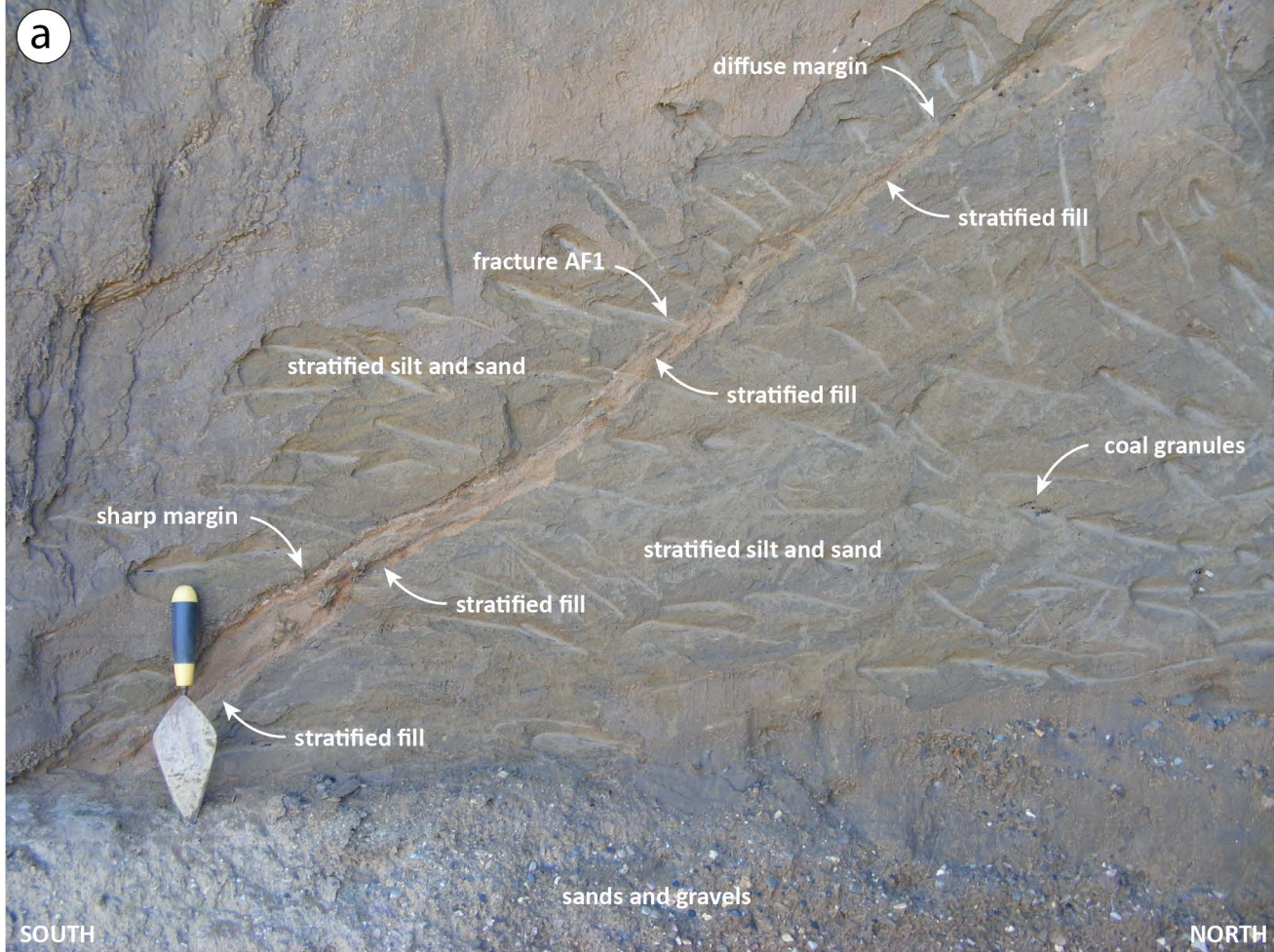


Figure 7 (a,b)

C

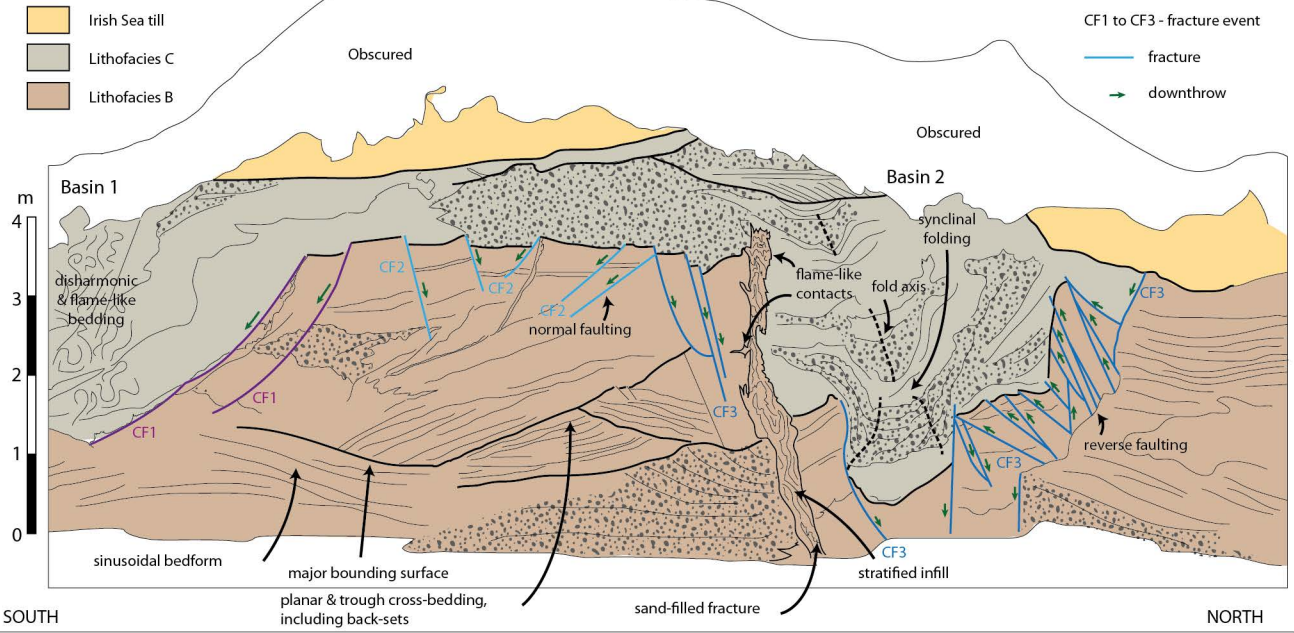
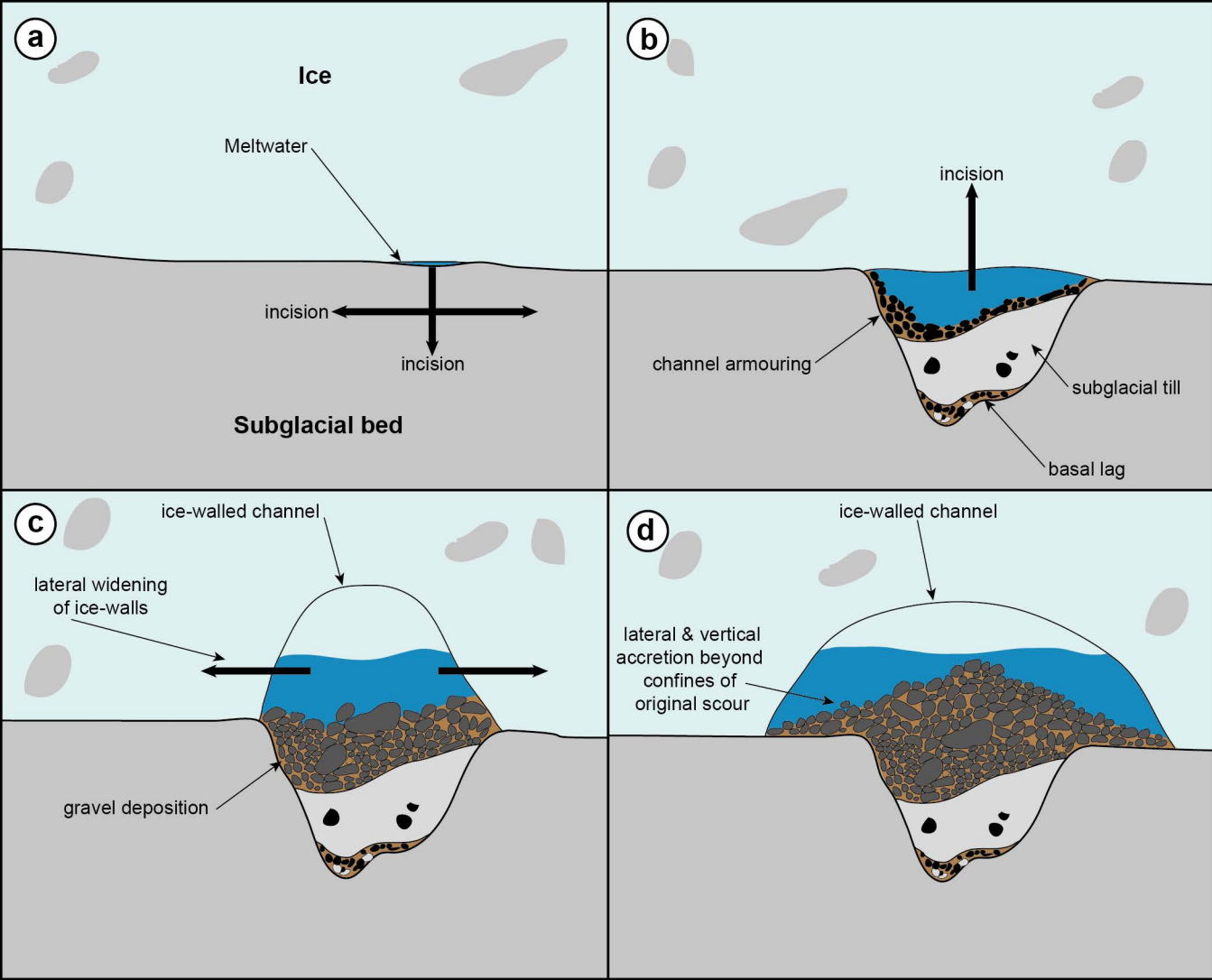


Figure 7c



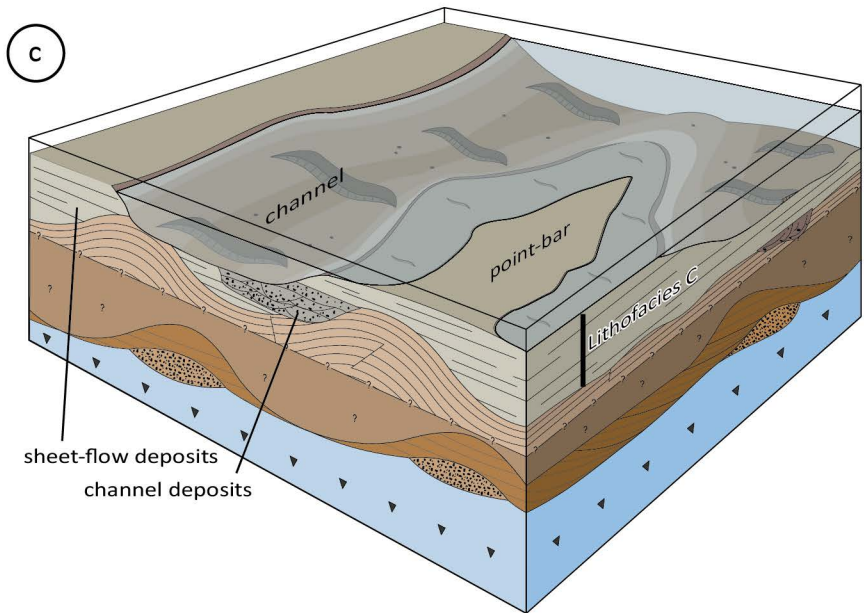
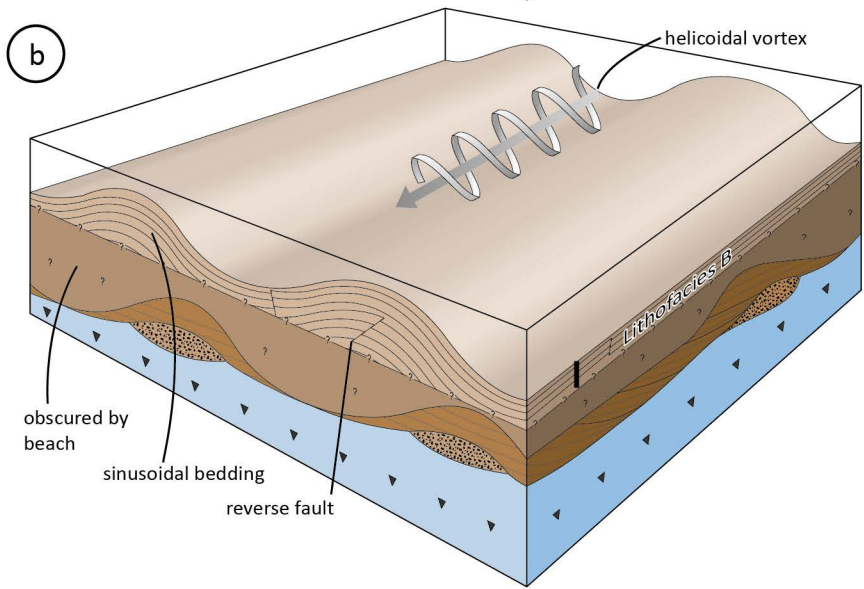
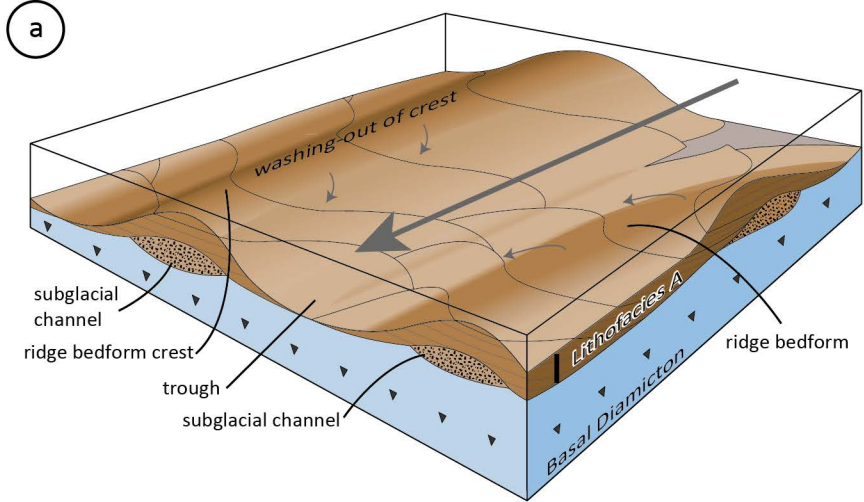
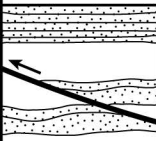


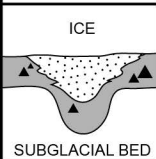
Figure 9

KEY INDICATORS



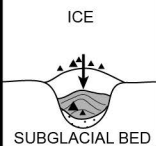
Syn-sedimentary Thrust & Reverse faults

Small-scale reverse and thrust faults provide evidence for shear stresses being transmitted via the channels walls (subglacial bed or ice) into sediment. Syn-sedimentary faulting demonstrates that deformation occurred during sediment deposi-



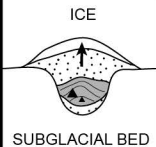
Subglacial Traction Till

Scours and channels containing subglacial traction till inter-bedded with the meltwater deposits. Care must be taken to ensure that the till-fill is not the product of bank collapse.



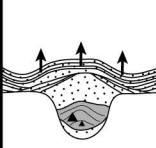
Melt-out diamicton

Scours and channels may contain diamicton derived from melt-out of debris-rich basal ice. Care must be taken to ensure the fill in not the product of bank collapse.



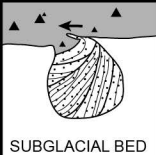
Vertically and laterally extending sediment bodies

Bodies of sediment (gravel or sand and gravel) that extend vertically and laterally beyond the confines of the host scour or channel imply lateral (ice-wall) constraint.



Sedimentary continuity

The continuity of sediments deposited by subglacial meltwater can potentially be an indicator providing a genetic and geometric link can be established between the various facies.



Glacitectonic overturning

Progressive syn-sedimentary overturning of older channel sediment-fills by subglacial shearing accompanied by down-ice shift in sedimentation. Upper bounding surface of channel fill may exhibit sub-horizontal shearing and intercalation with subglacial till.

Figure 10

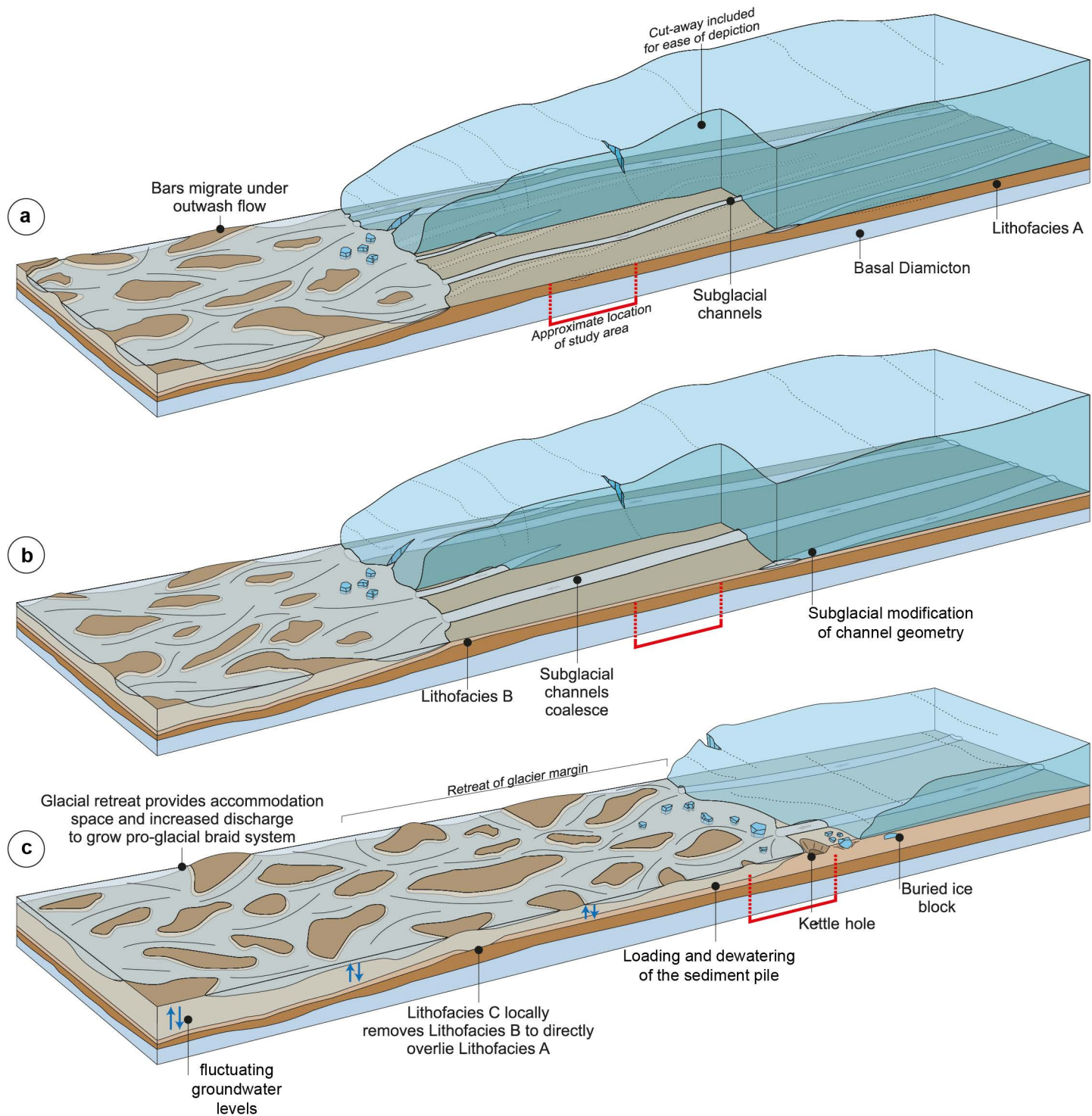


Figure 10

Appendix 1. Summary of the petrology of sand to fine-gravel sized sediments within the glacial outwash sequence exposed in the coastal cliff section at Lleiniog, Penmon Bay, north of Beaumaris, Anglesey, North Wales.

Sample	Grain size	Description	Clast assemblage dominant components	Minor to accessory components	Lithic clasts
PB 1.1	Fine- to medium-sand	Poorly sorted, texturally and compositionally immature sand comprising angular to subrounded, low sphericity clasts. Traces of a clay or hematitic rim cement	Monocrystalline quartz and sedimentary rock fragments	Polycrystalline quartz, opaque minerals, K-feldspar, plagioclase, epidote, cryptocrystalline quartz, microcline	Mudstone, sandstone, coal, siltstone, vein quartz
PB 1.2	Fine- to medium-sand	Poorly sorted, texturally and compositionally immature sand comprising subangular to subrounded, to occasionally well-rounded, low sphericity clasts. Traces of a clay or hematitic rim cement	Monocrystalline quartz and sedimentary rock fragments	Polycrystalline quartz, cryptocrystalline quartz, white mica, opaque minerals, plagioclase	Mudstone, coal, vein quartz, quartzose metamorphic rock, siltstone
PB 4.1	Coarse- to very coarse-sand to fine gravel	Lithic-rich, poorly to very poorly sorted, texturally and compositionally immature sand to fine gravel comprising angular to well-rounded, low sphericity clasts. Traces of a clay or hematitic rim cement	Sedimentary rock fragments	Polycrystalline quartz, monocrystalline quartz, clinopyroxene, opaque minerals, chlorite, carbonate	Mudstone, microgabbro, siltstone, wacke sandstone, litharenite, vein quartz, coal, indurated quartzose siltstone, feldspar phyric dacite/felsite, aphyric dacite/rhyolite, phyllite/micaceous schistose rock, very fine andesitic/basaltic rock, siltstone, cleaved mudstone
PB 4.1	Coarse- to very coarse-sand to fine gravel	Lithic-rich, poorly to very poorly sorted, texturally and compositionally immature sand to fine gravel comprising angular to well-rounded, low sphericity granule to small pebble sized clasts. Traces of a clay or hematitic rim cement	Sedimentary rock fragments	Carbonate, polycrystalline quartz, monocrystalline quartz, opaque minerals, chlorite, plagioclase	Mudstone, hematized mudstone, felsite/rhyolite, limestone, siltstone, altered sandstone, feldspar phyric felsite (cleaved), silicified felsite, altered andesitic/basaltic rock, bioclastic limestone, sericitised felsite, bioclastic micritic limestone, metabasaltic rock, polycrystalline carbonate rock, granitic rock
PB 5.1	Coarse- to very coarse-sand to fine gravel	Lithic-rich, very poorly sorted sand to fine gravel comprising angular to well-rounded, low sphericity clasts. Includes broken fragments of larger well-rounded grains (polycyclic)	Sedimentary rock fragments	Monocrystalline quartz, polycrystalline quartz, plagioclase, opaque minerals	Mudstone, cleaved mudstone, siltstone, wacke sandstone, bioclastic limestone, felsite/rhyolite, cleaved felsite/rhyolite, altered basalt, granitic rock, coal, indurated quartzose siltstone/fine sandstone
PB 5.2	Very coarse sand to fine	Poorly sorted, very poorly sorted sand to fine gravel comprising	Sedimentary rock fragments	Monocrystalline quartz, polycrystalline quartz, opaque minerals, carbonate, plagioclase	Mudstone, hematized mudstone, siltstone, wacke sandstone, felsite/rhyolite, granitic rock,

	gravel	angular to well-rounded, low sphericity clasts. Traces of a clay or hematitic rim cement			quartzite, hematized volcanic rock, limestone, micritic limestone
PB 6.1	Fine- to very coarse-sand	Very poorly sorted, texturally and compositionally immature sand comprising angular to well-rounded, low sphericity clasts	Sedimentary and very fine igneous rock fragments	Monocrystalline quartz, polycrystalline quartz, carbonate, opaque minerals	Mudstone, siltstone, silicified felsite, plagioclase-amphibole-phyric andesite, granitic rock, lapilli tuff rich in vitric shards, chloritised and silicified volcanic glass, calcareous siltstone, hematized mudstone, aphyric rhyolite/felsite, quartz-phyric rhyolite
PB 6.2	Very coarse-sand to fine gravel	Heterolithic, poorly sorted very coarse sand to fine gravel comprising angular to well-rounded, low sphericity clasts. Traces of a isopachous carbonate rim cement	Sedimentary rock fragments		Mudstone, bioclastic limestone, siltstone, polycrystalline quartz, altered rhyolite/felsite, bioclastic micritic limestone, andesite/basaltic rock, hematized mudstone
PB 7.1	Fine- to coarse sand	Poorly sorted, texturally and compositionally immature, quartzose and lithic-rich sand comprising angular to well-rounded, low sphericity clasts. Traces of a clay matrix derived from degraded mudstone rock fragments	Sedimentary rock fragments and monocrystalline quartz	Polycrystalline quartz, K-feldspar, opaque minerals, brachiopod spines, plagioclase, oxidised biotite	Mudstone, limestone, felsite, hematized mudstone, indurated quartzose siltstone/fine sandstone, fine wacke sandstone, siltstone, hematized volcanic rock
PB 7.2	Fine- to coarse-sand	Heterolithic, poorly sorted, texturally and compositionally immature quartzose sand comprising angular to well-rounded, low sphericity clasts. Traces of a clay matrix derived from degraded mudstone rock fragments. Traces of a clay or hematitic rim cement	Monocrystalline quartz and sedimentary rock fragments	Polycrystalline quartz, opaque minerals, carbonate, plagioclase	Mudstone, felsite/rhyolite, siltstone, hematized mudstone, limestone, altered basaltic rock, indurated quartz arenite, micrographic intergrowth, schistose metamorphic rock
PB 10.1	Very coarse sand to fine gravel	Poorly sorted, texturally and compositionally immature, heterolithic coarse sand to fine gravel comprising angular to well-rounded, low sphericity clasts	Sedimentary rock fragments	Polycrystalline quartz, monocrystalline quartz	Mudstone, bioclastic limestone, siltstone, quartzose metamorphic rock, cleaved volcanic rock, felsite/rhyolite
PB 10.2	Very coarse sand to fine gravel	Poorly sorted, texturally and compositionally, lithic-rich, heterolithic, immature sand to fine	Sedimentary rock fragments	Monocrystalline quartz, polycrystalline quartz, plagioclase, opaque minerals, carbonate, cryptocrystalline quartz	Mudstone, indurated quartz arenite, siltstone, hematized mudstone, bioclastic limestone, felsite/rhyolite, feldspar-quartz-phyric rhyolite,

		gravel comprising angular to well-rounded, low sphericity clasts. Traces of a carbonate cement present			granitic rock, fine wacke sandstone, metasedimentary rock, tuffaceous rock, litharenite
--	--	--	--	--	---

Appendix 2. Summary of the petrology of pebble to cobble sized clasts contained within the glacial outwash sequence exposed in the coastal cliff section at Lleiniog, Penmon Bay, north of Beaumaris, Anglesey, North Wales.

Sample	Rock Type	Description	Provenance
PB 5A	siltstone	Laminated, fine-grained, slightly calcareous quartzose siltstone with a matrix-poor, clast supported texture. Detrital micas (muscovite, biotite) are a common minor component	Triassic, or Carboniferous coal measures, or possibly ?Devonian sandstone sequences
PB 5B	quartz arenite	Fine- to medium-grained, indurated, compact, compositionally mature, moderately sorted, quartzose sandstone (quartz arenite) with a matrix-poor, clast-supported texture. Pressure solution and quartz overgrowths are the main mode of cementation, minor replacive carbonate cement noted	
PB 5C	sandstone	Reddened, fine-grained, compositionally immature, moderately to poorly sorted, quartzose sandstone with a hematitic rim cement and traces of a replacive carbonate cement. Detrital muscovite and biotite present	Triassic, or Carboniferous coal measures, or possibly ?Devonian sandstone sequences
PB 5D	feldspar phyrlic dacite (felsite)	Very fine-grained, hypocrySTALLINE, originally glassy (devitrified), weakly foliated, feldspar microporphyritic dacite (felsite) with a weakly developed cleavage. Foliation defined by lentils of quartz and feldspar.	Borrowdale Volcanic Group or ?Late Caledonian dyke swarm
PB 5E	pyroxene-plagioclase phyrlic metabasalt	Highly altered/metamorphosed (low grade) pyroxene-plagioclase (\pm olivine) microporphyritic meta basaltic rock. A pilotaxitic fabric is variably developed/preserved within the turbid groundmass. Secondary chlorite, epidote and opaque minerals	?Palaeogene dyke swarm
PB 5F	bioclastic limestone	Bioclastic limestone cut by several generations of carbonate veins. Contains brachiopod shell debris, foraminifera, calcispheres, echinoderm fragments	Carboniferous limestone
PB 5G	quartzose litharenite	Reddened, poorly sorted, immature, laminated, medium- to coarse-grained sandstone (quartzose litharenite) with a closely packed, clast-supported texture. Well-developed hematitic cement and pore-filling carbonate cement. Lithic clasts mainly schistose/quartzose metamorphic fragments	Triassic, or Carboniferous coal measures, or possibly ?Devonian sandstone sequences
PB 5H	feldspar phyrlic dacite (felsite)	Altered, weakly feldspar microporphyritic, hypocrySTALLINE, originally glassy (devitrified) dacite (felsite) with a weakly developed cleavage	Late Caledonian dyke swarm
PB 5I	bioclastic limestone (wackestone)	Bioclastic, micritic limestone (wackestone) containing thin shelled molluscs, foraminifera, echinoderm fragments, calcispheres, echinoderm spines, crinoid ossicles, brachiopod spines, algae	Carboniferous limestone
PB 5J	quartzose wacke sandstone	Fine- to medium-grained, poorly sorted, immature, heterolithic, quartzose wacke sandstone with a closely packed, clast-supported texture and a well-developed preferred alignment of clasts. Detrital garnet present	Lower Palaeozoic (Ordovician/Silurian) sandstone
PB 6A	siltstone to fine, silty sandstone	Fine-grained, poorly sorted, massive, compositionally mature, coarse-siltstone to fine-grained silty sandstone containing common detrital micas and replacive calcareous cement. Comparable to PB 5A	Triassic, or Carboniferous coal measures, or possibly ?Devonian sandstone sequences
PB 6B	fine-grained sandstone and siltstone	Reddened, laminated, moderately to poorly sorted, quartzose fine-grained sandstone and siltstone with a hematitic cement and minor	Triassic, or Carboniferous coal measures, or possibly ?Devonian sandstone

		replacive carbonate cement. Clast to cement supported texture	sequences
PB 6C	bioclastic micritic limestone (wackestone)	Bioclastic, micritic limestone (wackestone) cut by carbonate veins and containing thin shelled molluscs, foraminifera, echinoderm fragments, calcispheres, echinoderm spines, crinoid ossicles, brachiopod spines, gastropod fragments	Carboniferous limestone
PB 6D	bioclastic limestone (packstone)	Medium- to coarse-grained, bioclastic limestone (packstone) with a sparry carbonate cement replacing the original matrix. Containing thin shelled molluscs, foraminifera, echinoderm fragments, calcispheres, echinoderm spines, crinoid ossicles, brachiopod spines, algae. Cut by carbonate veins	Carboniferous limestone
PB 6E	granophyric granite	Medium-grained, inequigranular, holocrystalline, anhedral granular, aphyric granite characterised by a well-developed granophyric intergrowth. Contains xenoliths of finer grained granite. Composed of quartz, plagioclase and K-feldspar with traces of opaque minerals and chlorite	Ennerdale Microgranite Pluton
PB 6F	sandstone to coarse siltstone	Laminated, cross-laminated, fine-grained, indurated, quartzose sandstone to coarse-siltstone with a weakly developed cleavage	Lower Palaeozoic (Ordovician/Silurian) sandstone
PB 6G	biotite-muscovite-granite	Altered, inequigranular, holocrystalline, anhedral granular, biotite-muscovite-granite composed of quartz, K-feldspar, plagioclase, biotite and muscovite. Contains poikilitic intergranular microcline, weakly plagioclase porphyritic	Eskdale Granite Pluton
PB 6H	dacite/rhyolite (felsite)	Highly altered (carbonate replacement), aphyric, weakly foliated/cleaved, hypocrySTALLINE dacite/rhyolite (felsite) containing pseudomorphs after feldspar microlites	Borrowdale Volcanic Group or ?Late Caledonian dyke swarm
PB 6I	bioclastic limestone (packstone)	Bioclastic limestone with a complex diagenetic history including the development of a coarse sparry replacive carbonate cement which locally overprints original clastic texture. Contains echinoderm spines, echinoderm fragments, brachiopod shell fragments, thin walled mollusc shell fragments	Carboniferous limestone
PB 6J	bioclastic limestone (packstone/wackestone)	Bioclastic limestone with a finely crystalline/microcrystalline sparry carbonate matrix. Contains foraminifera, echinoderm spines, echinoderm fragments, brachiopod shell fragments, thin walled mollusc shell fragments, brachiopod spines, crinoid ossicles	Carboniferous limestone
PB 6K	rhyolitic lapilli-tuff	Altered, welded, rhyolitic lapilli-tuff containing feldspar and quartz crystals fragments and devitrifies/altered glass shards. Moderately to well-developed eutaxitic fabric defined by variably collapsed glassy lithic clasts	Borrowdale Volcanic Group
PB 6L	mudstone	Red-brown mudstone with optically aligned clay minerals defining a moderate to well-developed foliation (plasmic fabric). Patchy iron staining and disseminated opaque minerals present	Triassic, or Carboniferous coal measures, or possibly ?Devonian sandstone sequences
PB 6M	granophyric biotite-granite	Medium-grained, inequigranular, anhedral granular, holocrystalline biotite-granite with a well developed granophyric intergrowth. Comprises the assemblage quartz, plagioclase, K-feldspar and biotite	Ennerdale Microgranite Pluton
PB 6N	quartz-arenite	Fine- to medium-grained, compositionally mature, moderately to well-sorted, indurated quartzose sandstone (quartz-arenite) with a closely packed,	

		clast-supported texture. Pressure solution and quartz overgrowths form the main modes of cementation with traces of a replacive carbonate cement also present. Comparable to PB 5B	
PB 6O	silicified mudstone	Brecciated and silicified, red-brown mudstone comparable to PB 6L cut by a complex network of cryptocrystalline to microcrystalline quartz veins and minor carbonate veins. Possible cataclasis/fault breccia	?Triassic, or Carboniferous coal measures, or possibly ?Devonian sandstone sequences
PB 6P	bioclastic limestone (packstone)	Bioclastic limestone (packstone) showing evidence of early micritisation of bioclasts followed by later replacement by sparry carbonate. Cut by carbonate veins. Contains algae, shell fragments, echinoderm spines, echinoderm fragments and possible gastropod bioclasts	Carboniferous limestone
PB 10A	welded rhyolitic lapillituff	Parataxitic to eutaxitic, silicified, welded rhyolitic to dacitic lapillituff possessing a well-developed welding fabric. Originally glassy, now devitrified and contains fragments of feldspar crystals	Borrowdale Volcanic Group
PB 10B	quartz-arenite	Fine- to medium grained, poorly sorted, compositionally mature, quartzose sandstone with a closely packed, clast-supported texture. Pressure solution and quartz overgrowths main modes of cementation with traces of a replacive carbonate cement. Less indurated version of PB 6N	
PB 10C	quartz-arenite	Indurated, medium- to coarse-grained, compositionally mature, quartzose sandstone (quartz-arenite) with a closely packed, clast-supported texture. Pressure solution and quartz overgrowths main modes of cementation with traces of a replacive carbonate cement and opaque mineralisation/cement. Comparable to PB 10B	
PB 10D	quartz-arenite	Indurated, fine-grained, compositionally mature, quartzose sandstone (quartz-arenite) with a closely packed, clast-supported texture. Pressure solution and quartz overgrowths main modes of cementation with traces of a replacive carbonate cement. Comparable to PB 10B and 10C	
PB 10E	coarse litharenite to microconglomerate	Deformed, heterolithic, very coarse-grained, lithic-rich sandstone (litharenite) or microconglomerate with a micaceous silty matrix. Clast assemblage dominated by quartzose metamorphic/deformed rock fragments. Lithic clasts include quartz-chlorite-schist, vein quartz, quartzite, quartzose mylonitic rock, indurated quartzose sandstone, altered feldspar phyric basaltic rock fragments	
PB 10F	quartz-litharenite	Fine- to medium-grained, poorly sorted, compositionally and texturally immature, heterolithic, massive reddened, quartzose lithic-rich sandstone (quartz-litharenite).	Lower Palaeozoic (Ordovician/Silurian) sandstone
PB 10G	dacite/rhyolite (felsite)	Altered, fine-grained, hypocrySTALLINE, foliated, originally glassy dacite/rhyolite (felsite) with a well-developed pilotaxitic fabric. Devitrification resulted in the development of snowflake-like textures in the groundmass	Borrowdale Volcanic Group or ?Late Caledonian dyke swarm
PB 10H	feldspar phyric dacite	Fine-grained, hypocrySTALLINE, originally glassy (devitrified), foliated, cleaved, feldspar phyric dacite comparable to PB 10G. Contains carbonate (\pm chlorite) pseudomorphs after amphibole and/or biotite	Borrowdale Volcanic Group or ?Late Caledonian dyke swarm
PB 10I	Wacke sandstone	Fine-grained, texturally and compositionally	Lower Palaeozoic

		immature, massive, quartzose sandstone or wacke sandstone with a closely packed, clast-supported texture. Biotite a common minor detrital component. Traces of a replacive carbonate cement	sandstone or ?Siluro-Devonian sandstone (Midland Valley)
PB 10J	micritic, bioclastic limestone (wackestone)	Micritic to very finely microcrystalline, bioclastic limestone (wackestone) which possess a dusty looking micritic matrix with fine spots of microcrystalline carbonate. Contains brachiopod shell fragments, foraminifera, crinoid ossicles, echinoderm fragments, thin shell fragments. Evidence of early micritisation of bioclasts followed by sparry carbonate growth with traces of diagenetic quartz	Carboniferous limestone
PB 10K	Xenolithic biotite-granite	Medium-grained, holocrystalline, xenolithic, biotite-rich, titanite-bearing, biotite-granite/granodiorite containing rounded (?partially digested) co-magmatic xenoliths of a much finer grained granite. The xenoliths comprise an open framework of small plagioclase laths with interstitial/intersertal areas filled by quartz and feldspar which is a similar grain size to the host granite	
PB 10L	quartzose sandstone to wacke sandstone	Fine-grained, moderately sorted, texturally and compositionally immature, indurated, quartzose sandstone with a closely packed, clast-supported texture. Comparable to PB 10I	Lower Palaeozoic sandstone or ?Siluro-Devonian sandstone (Midland Valley)
PB 10M	bioclastic limestone (packstone)	Bioclastic limestone (packstone) containing evidence of early micritisation of bioclasts and later growth of sparry carbonate. Bioclasts include echinoderm fragments, crinoid ossicles, brachiopod fragments, foraminifera, brachiopod spines, thin shelled mollusc fragments. Minor dolomitisation and de-dolomitisation	Carboniferous limestone
1	biotite-granite	Altered, coarse-grained, inequigranular, anhedral granular, holocrystalline, microcline phyric biotite-granite with strained quartz. Comprising the assemblage quartz, K-feldspar, plagioclase, chloritised biotite and muscovite (?primary)	Cairnsmore of Fleet or Criffel-Dalbeattie Granite Pluton
2	foliated, plagioclase phyric, biotite-amphibole granodiorite	Foliated, medium-grained, anhedral granular, inequigranular, holocrystalline, plagioclase phyric, biotite-amphibole-granodiorite with a well-developed pre-full crystallisation fabric. Relict pyroxene in cores of amphibole crystals. Comprising mineral assemblage plagioclase, quartz, amphibole, biotite, K-feldspar and titanite	Criffel-Dalbeattie Granite Pluton
3	dedolomitised carbonate rock	Dedolomitised, iron stained, crystalline, coarse-grained carbonate rock	
4	muscovite-biotite-granite	Medium- to coarse-grained, inequigranular, holocrystalline, anhedral granular, weakly microcline and plagioclase phyric muscovite-biotite-granite. Traces of micrographic intergrowth. Comprising the assemblage quartz, K-feldspar, plagioclase, chloritised biotite and muscovite	Eskdale Granite Pluton
5	biotite-granodiorite	Inequigranular, holocrystalline, anhedral granular, weakly foliated biotite granodiorite/granite with strained quartz. Pre-full crystallisation fabric defined by biotite and aggregates of variably aligned plagioclase laths. Comprising the assemblage quartz, plagioclase, K-feldspar and biotite	Criffel-Dalbeattie Granite Pluton

6	biotite (± muscovite) granite	Coarse-grained, holocrystalline, anhedral granular, inequigranular, massive, biotite-?muscovite-granite containing traces of micrographic intergrowth. Possible primary muscovite. Comprising the assemblage quartz, K-feldspar, plagioclase, biotite and muscovite	Eskdale Granite Pluton
7	granite	Altered, inequigranular, anhedral granular, medium- to coarse-grained, holocrystalline granite with distinctive dusty looking reaction coronas enclosing irregular (partially resorbed) quartz and feldspar crystals	
8	foliated amphibole-biotite-granodiorite	Moderately foliated, inequigranular, anhedral granular, holocrystalline amphibole-biotite-granodiorite with large intergranular, poikilitic K-feldspar/microcline crystals. Pre-full crystallisation fabric defined by aligned plagioclase, biotite and amphibole crystals and aggregates. Comprising the assemblage plagioclase, quartz, biotite, K-feldspar and amphibole	Criffel-Dalbeattie Granite Pluton
9	brecciated siltstone	Brecciated/cataclased, dusty looking siltstone containing traces of opaque mineralisation and carbonate veins	
10	granophyric biotite-granite	Sericitised, fine- to medium-grained, inequigranular, anhedral granular, holocrystalline, granophyric biotite-granite with well-developed micrographic intergrowth	Ennerdale Microgranite Pluton
11	biotite-granite	Sericitised, massive, coarse-grained, anhedral granular, inequigranular, holocrystalline biotite-granite containing aggregates of secondary muscovite. Comprising the assemblage quartz, K-feldspar, plagioclase and biotite	Cairnsmore of Fleet or Criffel-Dalbeattie Granite Pluton
12	biotite-granodiorite	Coarse-grained, massive, inequigranular, anhedral granular, holocrystalline, massive to weakly foliated biotite granodiorite/granite. Comprising the assemblage plagioclase, quartz, K-feldspar, biotite, amphibole and titanite	Cairnsmore of Fleet or Criffel-Dalbeattie Granite Pluton
13	muscovite-biotite-granite	Fine- to medium-grained, massive, inequigranular, anhedral granular, holocrystalline, weakly microcline phyric muscovite-biotite-granite containing traces of micrographic intergrowth. Comprising the assemblage quartz, K-feldspar, plagioclase, biotite and muscovite	Eskdale Granite Pluton
14	muscovite-biotite-granite	Altered (sericitised), inequigranular, anhedral granular, holocrystalline, coarse-grained, massive to ?weakly foliated muscovite-biotite-granite. Comprising the assemblage quartz, K-feldspar, plagioclase, muscovite and biotite	Eskdale Granite Pluton
15	foliated, amphibole-biotite-granodiorite	Altered (chloritised, sericitised), inequigranular, plagioclase phyric, foliated, fine- to medium-grained amphibole-biotite-granodiorite. Pre-full crystallisation fabric defined by aligned plagioclase crystals. Comprising the assemblage quartz, plagioclase, biotite, K-feldspar and amphibole	Criffel-Dalbeattie Granite Pluton